

Equilibrium fluctuations of a quasi-spherical vesicle: role of the membrane dissipation

Petia M. Vlahovska^a and Rony Granek^b

^a *Engineering Sciences and Applied Mathematics, Northwestern University, Evanston, IL 60208, USA; E-mail: petia.vlahovska@northwestern.edu,*

^b *Avram and Stella Goldstein-Goren Department of Biotechnology Engineering, Dept. of Physics, and Ilse Katz Institute for Nanoscale Science and Technology, Ben-Gurion University of The Negev, Beer Sheva 84105, Israel*

(Dated: May 6, 2026)

We theoretically investigate the thermally-driven curvature and lipid density fluctuations of a quasi-spherical vesicle, accounting for the dissipation due to monolayer viscosity and intermonolayer friction. The theory predicts that membrane curvature makes long-wavelength undulations sensitive to membrane viscosity and speeds up the relaxation of the lipid density fluctuations. Implications for the dynamic roughness and Dynamic Structure Factor measurements of submicron liposomes on nano-second time scales are discussed. Specifically, a clear stretched-exponential relaxation regime may not exist, in contrast to the behavior of planar membranes for which an anomalous diffusion exponent of $2/3$ has been predicted [Zilman and Granek, Phys. Rev. Lett. (1996)].

I. INTRODUCTION

The biological function of membranes is closely tied to their flexibility [1], commonly assessed through thermally driven undulations [2–9]. The canonical problem of curvature fluctuations of a membrane (flickering) was considered in the pioneering work by Brochard and Lennon [10]. In this minimal model, the membrane is considered a structureless interface with bending rigidity κ ; an undulation with wavenumber q of an initially planar membrane is dissipated by the viscosity of the surrounding fluid η and relaxes exponentially with a rate $\kappa q^3/4\eta$.

The undulation dynamics changes when the membrane itself is curved [11–20], since in-plane and out-of-plane displacements couple [13]. For a quasi-spherical, tensionless vesicle, whose shape is described in terms of fluctuating spherical harmonics modes $r_s(\phi, \theta, t) = R(1 + f(\phi, \theta, t))$, $f = \sum f_{\ell m}(t)Y_{\ell m}(\phi, \theta)$, the relaxation rate of a mode amplitude $f_{\ell m}$ is predicted to be (in the case of a structureless membrane and same fluid inside and outside the vesicle) [11–13, 19]

$$\hat{\omega} = \frac{\kappa}{\eta R^3} \frac{(\ell - 1)\ell^2(\ell + 1)^2(\ell + 2)}{4\ell^3 + 6\ell^2 - 1 + (4\ell^2 + 4\ell - 8)\chi_s}, \quad (1)$$

where $\chi_s = \eta_s/R\eta$ is a dimensionless membrane viscosity parameter, the ratio of the Saffman-Delbrück length (η_s/η) to the vesicle radius R ; here η_s and η are the membrane and bulk viscosities. Setting $\chi_s = 0$ reduces Eq. [1] to the result for a non-viscous vesicle [21]. For $\chi_s \gg 1$, a new regime is predicted to emerge in the relaxation spectrum of long-wavelength undulations, $1 \ll j \ll \chi_s$, in which dissipation is dominated by membrane viscosity and $\hat{\omega}(\ell) \simeq \frac{\kappa}{4\chi_s\eta R^3} \ell^4$. Provided this asymptotic regime is attained, the corresponding anomalous diffusion (stretching) exponent α , governing the membrane dynamic roughness and the dynamic structure factor (DSF), $S(k, t) \sim \exp[-(\Gamma_k t)^\alpha]$ —as measured in scattering experiments such as neutron spin echo (NSE) [22], dynamic light scattering [23], X-ray photon correlation spectroscopy [24], and fluctuation spectroscopy [25, 26]—becomes $\alpha = 1/2$, with $\Gamma_k \sim (k_B T)^2 k^4 R^2 / (\kappa \eta_s)$. This contrasts with the $\alpha = 2/3$ scaling and $\Gamma_k \sim (k_B T)^{3/2} k^3 / (\kappa^{1/2} \eta)$ predicted for large planar membranes [27] and vesicles [28] in the limit of negligible membrane viscosity, where $\hat{\omega}(\ell) \simeq \frac{\kappa}{4\eta R^3} \ell^3$ for $\ell \gg 1$. These predictions were recently experimentally confirmed in flickering of giant unilamellar vesicles [29], and also appear to apply to NSE data [30].

The minimal, zero-thickness membrane model captures the membrane dynamics only to a limited extent because it neglects the bilayer architecture of the membrane. More realistic approaches treat the membrane as an elastic thin plate, introducing corrections to account for finite thickness [31], or model it as a bilayer composed of two monolayers that can slide relative to each other. [32–34]. Bending the membrane stretches and compresses the outer and inner monolayers [35]. If monolayer slippage is allowed, the relaxation of the resulting lipid density difference, driven by monolayer compressibility and dissipated by lateral lipid flow and intermonolayer friction, has been shown to strongly affect the undulation dynamics of planar membranes at short times and wavelengths (submicron and nanoseconds) [3, 32, 36, 37], relevant to neutron spin echo and dynamic light scattering experiments [8, 38]. However, even in that case, the relaxation rate of the bending mode of a planar membrane asymptotically remains of the same form as the Brochard and Lennon result with bending rigidity κ replaced by the unrelaxed bending modulus $\tilde{\kappa} = \kappa + 2K_m d^2$ for deformations measured at the bilayer midplane in the absence of any slip [3, 32]; here K_m is the monolayer compression modulus and d is the monolayer thickness. The DSF stretching exponent of $2/3$ also remains unchanged

[3, 36]. This behavior is often assumed to hold over the typical NSE time and length scales, effectively presuming that the system has reached its asymptotic relaxation regime [3, 36]. This raises the question: Is this assumption justified for liposomes? Is there an effect of the spherical geometry?

Eq. [1] shows that, for a quasi-spherical vesicle, the relaxation of long-wavelength undulations is dominated by membrane viscosity when the Saffman–Delbrück length exceeds the radius of curvature, i.e., $\chi_s \geq 1$. However, the zero-thickness model does not account for lipid density fluctuations. Here, we extend the framework for the fluctuation dynamics of a quasi-spherical vesicle [33] to incorporate both intermonolayer friction and lipid density fluctuations, while also including membrane viscosity under the assumption that the monolayers behave as Newtonian fluids. The resulting theory provides a unified description of bilayer dynamics across experimentally relevant length and time scales.

II. PROBLEM STATEMENT

A. Membrane model

The fluid bilayer membrane consists of two monolayers of amphiphilic molecules—typically lipids or polymers [39, 40]. It exhibits a unique solid-fluid duality: it behaves as an elastic material in response to out-of-plane (bending) deformations, yet flows like a two-dimensional fluid under in-plane shear. The resistance to bending originates from the monolayers' finite thickness: changes in curvature compress one monolayer while stretching the other – in addition to bending each monolayer – incurring an additional elastic energy cost [41, 42]. In contrast, because the bilayer is held together by non-covalent bonds, the lipids are free to rearrange and flow laterally within the monolayer..

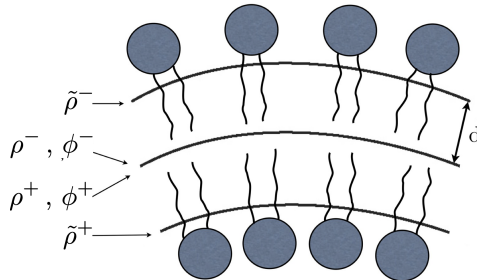


FIG. 1: **Structure of a lipid membrane formed by two identical monolayers.** At the bilayer neutral surface bending and stretching are decoupled. ρ^\mp are the monolayers densities, $\tilde{\rho}^\mp$, projected onto the neutral surface. $\tilde{\rho}^\mp = \rho^\mp(1 \pm 2dH)$, where d is the monolayer thickness and H is the mean curvature.

1. Membrane elastic energy and forces

We consider a membrane composed of two identical monolayers with neutral surfaces that are distance $2d$ apart, see Fig. 1 [32, 39]. Compression and expansion of the monolayers adds to the bending energy

$$\mathcal{H} = \frac{\kappa}{2} \int (2H)^2 dA + \sigma_0 \int dA + \frac{K_m}{2} \int [(\phi^- + 2dH)^2 + (\phi^+ - 2dH)^2] dA, \quad (2)$$

where the integration is over the vesicle area A_0 (defined by the neutral surface), κ is the bending modulus (twice the monolayer bending modulus), $H = -\frac{1}{2}\nabla \cdot \mathbf{n}$ is the mean curvature (\mathbf{n} being the outward pointing normal), σ_0 is the membrane tension, K_m is the monolayer compressibility modulus, $\phi^\pm = \rho^\pm/\rho_0 - 1$, and the average equilibrium lipid density is $\rho_0 = (\rho_0^+ + \rho_0^-)/2$, $\rho_0^\pm = N^\pm/A_0$. Eq. [2] is rewritten as

$$\mathcal{H} = \frac{\tilde{\kappa}}{2} \int (2H)^2 dA + \sigma_0 \int dA + 2dK_m \int H(\phi^- - \phi^+) dA + \frac{K_m}{2} \int (\phi^+)^2 dA + \frac{K_m}{2} \int (\phi^-)^2 dA, \quad (3)$$

The parameter $\tilde{\kappa} = \kappa + 2d^2K_m$ is a renormalized bending rigidity and represents the bending modulus for deformations measured at the bilayer midplane in the absence of any density relaxation. The elastic terms have been expanded

and grouped to give the third term which describes the energy cost associated with the coupling between changes in curvature and local lipid densities [32, 33].

A non-equilibrium membrane configuration, \mathbf{r}_s , exerts a force on the surrounding fluid, $\mathbf{t} = -\delta\mathcal{H}/\delta\mathbf{r}_s$ [43]. The bending component for each monolayer is

$$\mathbf{t}_\kappa^\pm = \tilde{\kappa} [2H(H^2 - K_G) + \nabla_s^2 H] \mathbf{n} \quad (4)$$

where K_G is the Gaussian curvature, ∇_s is the surface gradient operator, and ∇_s^2 is the Laplace-Beltrami operator. Each monolayer experiences tension $\sigma^\pm = \frac{1}{2}\sigma_0 - K_m\phi^\pm - \frac{K_m}{2}(\phi^\pm)^2$, which gives rise to tractions

$$\mathbf{t}_\sigma^\pm = -\sigma^\pm (2H) \mathbf{n} - \nabla_s \sigma^\pm \quad (5)$$

The curvature-lipid density coupling gives rise to additional forces [33]

$$\mathbf{t}_c^\pm = \mp 2dK_m \left(\frac{1}{2} \nabla_s^2 \phi^\pm + (2H^2 - K_G)\phi^\pm + 2H^2 \right) \mathbf{n} \mp 2dK_m (1 + \phi^\pm) \nabla_s H. \quad (6)$$

2. Dissipation in the membrane

The weak intermolecular interactions between the two monolayers allow the two monolayers to slide over each other [44–46], thereby making the tangential component of the velocity discontinuous. The friction due to the relative motion gives rise to surface stresses on the monolayers facing the inner fluid (+) and the outer fluid (–)

$$\mathbf{t}_b^\pm = \mp b(\mathbf{v}_t^- - \mathbf{v}_t^+), \quad (7)$$

where the parameter b is the slip coefficient. Its magnitude varies greatly depending on the type of lipid; values of b have been reported in the range $10^4 - 10^9$ N.s/m³ [47–49].

Assuming the monolayers behave as Newtonian fluids, the viscous stresses are given by the Boussinesq-Scriven equation [50]

$$\boldsymbol{\tau}_v = \nabla_s \cdot [(\eta_{md} - \eta_m) (\mathbf{I}_s : \mathbf{D}_s) \mathbf{I}_s + 2\eta_m \mathbf{D}_s], \quad (8)$$

where η_m and η_{md} are the 2D shear and dilatational monolayer viscosities; for a symmetric bilayer, the corresponding membrane viscosities are $\eta_s = 2\eta_m$ and $\eta_d = 2\eta_{md}$. $\mathbf{I}_s = \mathbf{I} - \mathbf{nn}$, \mathbf{I} is the three-dimensional idemfactor, and the surface rate-of-strain tensor is

$$\mathbf{D}_s = \frac{1}{2} \left[\nabla_s \mathbf{v}_s \cdot \mathbf{I}_s + \mathbf{I}_s \cdot (\nabla_s \mathbf{v}_s)^\dagger \right], \quad (9)$$

where the superscript \dagger denotes transpose. Note that in general the velocity of a deforming interface, \mathbf{v}_s , has both a normal and a tangential component to the interface, $\mathbf{v}_s = v_n \mathbf{n} + \mathbf{v}_t$.

The viscous interfacial tractions derived from Eq. [8] [50–52] have in general complicated expressions. These simplify in the case of a sphere

$$\mathbf{t}_v^\pm = -\eta_{md} \frac{2}{R} (\nabla_s \cdot \mathbf{v}_s^\pm) \hat{\mathbf{r}} + (\eta_{md} + \eta_m) \nabla_s \nabla_s \cdot \mathbf{v}_s^\pm + \eta_m \left(\hat{\mathbf{r}} \times \nabla_s ((\nabla_s \times \mathbf{v}_s^\pm) \cdot \hat{\mathbf{r}}) - \frac{2}{R} (\nabla_s \mathbf{v}_s^\pm) \cdot \hat{\mathbf{r}} \right) \quad (10)$$

where on a sphere with radius R , $\nabla_s \cdot \mathbf{v}_s = \nabla_s \cdot \mathbf{v}_t + 2v_n/R$, $H = -1/R$ and $K_G = 1/R^2$.

Data for membrane viscosities are scarce, and reported values vary greatly [53, 54]. Typical membrane shear viscosities for unsaturated lipids in the fluid phase obtained from micron-sized GUVs are on the order of $\eta_s \sim 10^{-9}$ N.s/m [53], although values obtained from molecular dynamic simulations of ~ 10 nm membrane patches could be two orders of magnitude lower [54, 55]. Membranes in the liquid-ordered phase [29] or those composed of polymers [53, 56] can exhibit significantly higher viscosities. Measurements of the dilatational viscosity are even more limited [57, 58], but the most recent reports indicate that dilatational and shear viscosities are of comparable magnitude [59].

3. Dissipation in the bulk and fluid-membrane coupling

Let us consider a vesicle suspended in a fluid with viscosity η^- and enclosing fluid with viscosity η^+ ; both fluids are assumed incompressible and Newtonian. Fluid motion at the lengthscales of a micron-sized vesicle and smaller is

in the overdamped regime, where inertia effects are negligible. Accordingly, the fluid velocity \mathbf{v} and pressure p obey the Stokes equations

$$\nabla \cdot \mathbf{T}^\pm = -\nabla p^\pm + \eta^\pm \nabla^2 \mathbf{v}^\pm = 0, \quad \nabla \cdot \mathbf{v}^\pm = 0, \quad (11)$$

where \mathbf{T} is the bulk hydrodynamic stress tensor

$$\mathbf{T} = -p\mathbf{I} + \eta [\nabla \mathbf{v} + (\nabla \mathbf{v})^\dagger]. \quad (12)$$

We will use a reference frame centered at the vesicle. At the membrane, the normal component of the velocity is continuous (assuming an impermeable membrane), $\mathbf{v}^+ \cdot \mathbf{n} = \mathbf{v}^- \cdot \mathbf{n} \equiv \mathbf{v}_s \cdot \mathbf{n}$, where \mathbf{n} is the outward pointing unit normal vector. The vesicle deformation is determined from the kinematic condition at the interface

$$\frac{\partial \mathbf{r}_s}{\partial t} = \mathbf{v}_s, \quad (13)$$

where \mathbf{r}_s is the position vector of the neutral surface of the bilayer.

Mechanical equilibrium at each monolayer surface requires

$$\mathbf{t}^{\text{hd},\pm} = \mathbf{t}_\kappa^\pm + \mathbf{t}_\sigma^\pm + \mathbf{t}_c^\pm + \mathbf{t}_v^\pm \mp b(\mathbf{v}_t^- - \mathbf{v}_t^+), \quad (14)$$

where $\mathbf{t}^{\text{hd},\pm} = \mp \mathbf{n} \cdot \mathbf{T}^\pm$ are the hydrodynamic tractions. This boundary condition can be expressed alternatively as

$$\mathbf{t}^{\text{hd},-} - \mathbf{t}^{\text{hd},+} = \mathbf{t}_s^\Delta, \quad \mathbf{t}^{\text{hd},-} + \mathbf{t}^{\text{hd},+} = \mathbf{t}_s^\Sigma, \quad (15)$$

where \mathbf{t}_s^Σ and \mathbf{t}_s^Δ are the sum and difference of the membrane tractions on the right-hand side of Eq. [14].

4. Nondimensionalization

Henceforth, all variables are non-dimensionalized using the radius of a sphere with the same volume as the vesicle, the viscosity of the suspending (outer) fluid, and the characteristic bending stress $\tau_c = \tilde{\kappa}/R^3$. Accordingly, the time scale is $t_c = \eta^-/\tau_c$ and the velocity scale is $V_c = R\tau_c/\eta^-$. The membrane elastic and dissipative stresses give rise to the following dimensionless parameters

$$\alpha = \frac{K_m R^2}{\tilde{\kappa}}, \quad \lambda = \frac{2K_m d R}{\tilde{\kappa}}, \quad (16)$$

$$\chi_s = \frac{\eta_s}{\eta^- R}, \quad \chi_d = \frac{\eta_d}{\eta^- R}, \quad \beta = \frac{bR}{\eta^-}, \quad \chi = \frac{\eta^+}{\eta^-}$$

III. DYNAMICS OF A QUASI-SPHERICAL VESICLE

Let us consider a vesicle with total area A_0 of the neutral surface, and enclosing fluid volume V . The asphericity (deflation) of the vesicle is characterized by a dimensionless excess area

$$\Delta = A_0/R^2 - 4\pi, \quad (17)$$

where the characteristic vesicle size R is defined by the radius of a sphere of the same volume, $R = (3V/4\pi)^{1/3}$. We will consider a quasi-spherical vesicle for which $\Delta \ll 1$ and the excess area is stored in thermal undulations. In this case, the instantaneous vesicle shape parametrized relative to a reference sphere centered at the vesicle center of mass is

$$r_s = R(1 + f(\theta, \varphi, t)), \quad (18)$$

where $f \ll 1$ are the amplitude of the membrane undulations, whose magnitude is set by the competition of the thermal noise and resistance to bending. Considering that $\langle f^2 \rangle \simeq k_B T / (12\pi\kappa)$ [28], this implies that for $\kappa \gtrsim k_B T$ our linear analysis is reasonable. The r , θ and φ are the radial distance, polar and azimuthal angles in a spherical coordinate system.

The shape evolution is determined from the kinematic condition Eq. [13]

$$\frac{\partial f}{\partial t} = \mathbf{v}_s \cdot \nabla f. \quad (19)$$

Since there is no exchange of lipids between the monolayers and between the monolayers and the bulk fluids, the total number of lipids in each monolayer is conserved

$$\frac{\partial \rho^\pm}{\partial t} + \nabla_s \cdot (\mathbf{v}_t^\pm \rho^\pm) + \rho^\pm (\nabla_s \cdot \mathbf{n})(\mathbf{v}_s \cdot \mathbf{n}) = 0 \quad (20)$$

At equilibrium, the lipid density is $\rho_0^\pm/\rho_0 = 1 + \phi_0^\pm = 1 \mp \phi_0$, where

$$\phi_0 = \frac{\rho_0^- - \rho_0^+}{2\rho_0} = \frac{N^- - N^+}{N^- + N^+}$$

is a measure of the equilibrium asymmetry in the lipid numbers of the monolayers: on a sphere equal lipid density of the monolayers implies different lipid numbers because the area of the outer monolayer is greater than the inner monolayer; for a sphere with radius R and distance between the monolayers surfaces $2d$, $A_- \approx A_+ (1 + 2d/R)$, i.e., $\phi_0 = 2d/R$.

For small perturbations about the equilibrium lipid density, $\rho^\pm/\rho_0 = \rho_0^\pm/\rho_0 + \phi^\pm$, the lipid transport equation becomes

$$\frac{1}{1 \mp \phi_0} \frac{\partial \phi^\pm}{\partial t} + \nabla_s \cdot \mathbf{v}_t^\pm + (\nabla_s \cdot \mathbf{n})(\mathbf{v}_s \cdot \mathbf{n}) = 0. \quad (21)$$

A. Solution

1. Vesicle shape and energy

Due to the spherical geometry of the problem, the vesicle shape and monolayer densities are expanded in spherical harmonics (see Appendix A for definitions)

$$f(\theta, \varphi, t) = \sum_{\ell m} f_{\ell m} Y_{\ell m}, \quad \phi^\pm = \phi_{00}^\pm + \sum_{\ell m} \phi_{\ell m}^\pm Y_{\ell m}, \quad (22)$$

where the sum denotes $\sum_{\ell m} \equiv \sum_{\ell=2}^{\infty} \sum_{m=-\ell}^{\ell}$. It is more convenient to work with the two alternative fields, the lipid density difference between the monolayers and the average lipid density

$$\phi = \frac{1}{2} (\phi^- - \phi^+), \quad \bar{\phi} = \frac{1}{2} (\phi^- + \phi^+), \quad (23)$$

which are expanded as follows

$$\phi = \phi_0 + \sum_{\ell m} \psi_{\ell m} Y_{\ell m}, \quad \bar{\phi} = \sum_{\ell m} \xi_{\ell m} Y_{\ell m} \quad (24)$$

Note that $\bar{\phi}_0 = (\phi_0^- + \phi_0^+)/2 = 0$ and $\phi_0 = (\phi_0^- - \phi_0^+)/2 = (N^- - N^+)/ (N^- + N^+) = \pm \phi_0^\mp$. The energy Eq. [3] expanded in spherical harmonics, is

$$\mathcal{H} = \frac{\tilde{\kappa}}{2} \sum_{\ell m} \left(\begin{pmatrix} f_{\ell m} \\ \psi_{\ell m} \end{pmatrix}^\dagger \cdot \mathbf{E} \cdot \begin{pmatrix} f_{\ell m}^* \\ \psi_{\ell m}^* \end{pmatrix} + 2\alpha \xi_{\ell m}^2 \right)$$

where

$$\begin{aligned} E_{11} &= (\ell - 1)(\ell + 2) (\ell(\ell + 1) + \bar{\sigma}_0 - \alpha \phi_0^2), \\ E_{12} = E_{21} &= -(\ell - 1)(\ell + 2)\lambda, \\ E_{22} &= 2\alpha. \end{aligned} \quad (25)$$

$\bar{\sigma}_0 = \sigma_0 R^2 / \tilde{\kappa}$ corresponds to the tension of a planar membrane, and for a sphere, $\phi_0 = 2d/R$, if the lipid density is the same for both monolayers. From the equipartition theorem

$$\langle f_{\ell m}^2 \rangle = \frac{k_B T}{\tilde{\kappa}} \frac{E_{22}}{E_{11}E_{22} - E_{12}E_{21}} = \frac{k_B T}{(\ell(\ell+1) - 2)(\ell(\ell+1)\kappa + \sigma_0 R^2)} \quad (26)$$

$$\langle \psi_{\ell m}^2 \rangle = \frac{k_B T}{\tilde{\kappa}} \frac{E_{11}}{E_{11}E_{22} - E_{12}E_{21}} = k_B T \frac{(\ell(\ell+1)\tilde{\kappa} + \sigma_0 R^2 - 4K_m d^2)}{2K_m R^2 (\ell(\ell+1)\kappa + \sigma_0 R^2)} \quad (27)$$

$$\langle f_{\ell m} \psi_{\ell m}^* \rangle = \frac{k_B T}{\tilde{\kappa}} \frac{E_{12}}{E_{12}E_{21} - E_{11}E_{22}} = k_B T \frac{d}{R(\ell(\ell+1)\kappa + \sigma_0 R^2)} \quad (28)$$

$$\langle \xi_{\ell m} \xi_{\ell m}^* \rangle = \frac{k_B T}{2K_m R^2} \quad (29)$$

2. Flow

To solve for the flow, we use the basis of fundamental solutions of the Stokes equations in a spherical geometry [19, 60, 61], listed in Appendix D,

$$\mathbf{v}^- = \sum_{\ell m q} c_{\ell m q}^- \mathbf{u}_{\ell m q}^-(\mathbf{r}), \quad \mathbf{v}^+ = \sum_{\ell m q} c_{\ell m q}^+ \mathbf{u}_{\ell m q}^+(\mathbf{r}). \quad (30)$$

q takes values 0, 1, and 2. The functions $\mathbf{u}_{\ell m q}^\pm$ are vector solid spherical harmonics related to the harmonics in the Lamb solution. With respect to a sphere, $\mathbf{u}_{\ell m 0}^\pm$ is radial, while $\mathbf{u}_{\ell m 1}^\pm$ and $\mathbf{u}_{\ell m 2}^\pm$ are tangential; $\mathbf{u}_{\ell m 1}^\pm$ is surface-solenoidal ($\nabla_s \cdot \mathbf{u}_{\ell m 1}^\pm = 0$). The velocity coefficients $c_{\ell m q}^\pm$ are determined from the condition for velocity continuity and the stress balance.

3. Shape and lipid density evolution

The shape evolution equation, Eq. [19], to a leading order is

$$\dot{f}_{\ell m} = c_{\ell m 2}^+ = c_{\ell m 2}^-. \quad (31)$$

Here the dot denotes a time derivative. The redistribution of the lipids Eq. [21] yields

$$\begin{aligned} \dot{\psi}_{\ell m} &= -2\phi_0 \dot{f}_{\ell m} + \frac{1}{2} \ell(\ell+1) ((1+\phi_0) c_{\ell m 0}^- - (1-\phi_0) c_{\ell m 0}^+), \\ \dot{\xi}_{\ell m} &= -2\dot{f}_{\ell m} + \frac{1}{2} \ell(\ell+1) ((1+\phi_0) c_{\ell m 0}^- - (1-\phi_0) c_{\ell m 0}^+) \end{aligned} \quad (32)$$

We neglect lipid flip-flop and thus the total number of lipids in each monolayer is constant. An examination of the characteristic time scales corresponding to relaxation of perturbations in the curvature and monolayer density – bending limited by solvent viscous dissipation (t_κ), and monolayer compression/expansion limited by either sliding friction between the monolayers (t_b) or lateral lipid flow (t_K) – shows that

$$t_\kappa = \frac{\eta^- R^3}{\kappa} \sim 12\text{s}, \quad t_b = \frac{bR^2}{K_m} \sim 0.05\text{s}, \quad t_K = \frac{\eta^- R}{K_m} \sim 5 \times 10^{-7}\text{s}, \quad (33)$$

for a GUV with radius $R = 10^{-5}$ m, where $\eta^- = 0.001$ N.s/m², $\kappa = 20k_B T$, $K_m = 0.02$ N/m, and $b = 10^7$ N.s/m³ [32]. Even for liposomes with submicron radius, the time scale for the average density relaxation remains much faster than the relaxation of the bending and lipid density fluctuations (for example, for a $R = 50$ nm, $t_\kappa \sim t_b \sim 1\mu\text{s}$, $t_{K_m} \sim 2\text{ns}$). The large separation of time scales allows us to set [33, 62],

$$\dot{\xi}_{\ell m} = 0. \quad (34)$$

This condition is analogous to the ‘‘local area incompressibility’’ constraint used in the zero-thickness model. It means that local changes in the average of the projected densities relax faster than changes in shape or local density difference [62]. As pointed out in [33] this constraint is not to be directly compared to incompressibility of the bulk fluids because only one mode of monolayer density relaxation, $\xi_{\ell m}$, can be eliminated by invoking it ($\psi_{\ell m}$ remains). This added condition is treated as an extra constraint in the system which has to be explicitly enforced.

Setting $\dot{\xi}_{\ell m} = 0$ in Eq. [32], solving for $c_{\ell m 0}^-$ yields

$$c_{\ell m 0}^+ = \frac{1}{1 - \phi_0} \left(\frac{4f_{\ell m}}{\ell(\ell + 1)} - c_{\ell m 0}^-(1 + \phi_0) \right) \quad (35)$$

Inserting this result in the expression for $\dot{\psi}_{\ell m}$ leads to

$$\dot{\psi}_{\ell m} = -(1 + \phi_0) \left(2\dot{f}_{\ell m} + \ell(\ell + 1)c_{\ell m 0}^- \right) \quad (36)$$

4. Interfacial stresses

For a quasi-spherical vesicle, we consider small deviations from equilibrium, $H = -1 - C$ and $K = 1 + 2C$, see Eq. [C20] and Eq. [C21], $\phi^\pm = \phi_0^\pm + \tilde{\phi}^\pm$, and the $\sigma^\pm = \bar{\sigma}^\pm + \tilde{\sigma}^\pm$ where

$$\bar{\sigma}^\pm = \frac{\sigma_0}{2} - \alpha\phi_0^\pm - \frac{\alpha}{2}(\phi_0^\pm)^2, \quad \tilde{\sigma}^\pm = -\alpha\tilde{\phi}^\pm - \alpha\phi_0^\pm\tilde{\phi}^\pm$$

To the linear order in the shape and lipid density deviations from equilibrium, the radial components of the membrane elastic tractions Eq. [4] and Eq. [6] are

$$\begin{aligned} \mathbf{t}_\kappa^\pm \cdot \mathbf{n} &\approx -2\nabla_s^2 C, & \mathbf{t}_\sigma^\pm \cdot \mathbf{n} &\approx 2\bar{\sigma} + 2\tilde{\sigma}, \\ \mathbf{t}_c^\pm \cdot \mathbf{n} &\approx \mp\lambda \left(\frac{1}{2}\nabla_s^2 \tilde{\phi}^\pm + \tilde{\phi}^\pm + 2\phi_0^\pm C + 4C \right) \end{aligned} \quad (37)$$

where constant terms are omitted since these are balanced by hydrostatic pressure. The tangential tractions are

$$\mathbf{t}_t^\pm = -\nabla_s \sigma^\pm \mp \lambda(1 + \phi^\pm) \nabla_s H \approx (1 + \phi_0^\pm) \left(\alpha \nabla_s \tilde{\phi}^\pm \pm \lambda \nabla_s C \right) \quad (38)$$

In terms of spherical harmonics, the interfacial stresses are written as

$$\mathbf{t} \cdot \hat{\mathbf{r}} = \tau_{\ell m 2} Y_{\ell m}, \quad \mathbf{t}_t = \tau_{\ell m 0} \nabla_s Y_{\ell m}. \quad (39)$$

The tangential tractions derived from Eq. [38] are

$$\begin{aligned} \tau_{j m 0}^\Sigma &= \tau_{j m 0}^- + \tau_{j m 0}^+ = 2\alpha (\xi_{\ell m} + \phi_0 \psi_{\ell m}) - \lambda \phi_0 (\ell + 2)(\ell - 1) f_{\ell m} \\ \tau_{j m 0}^\Delta &= \tau_{j m 0}^- - \tau_{j m 0}^+ = 2\alpha (\psi_{j m} + \phi_0 \xi_{\ell m}) - \lambda (\ell + 2)(\ell - 1) f_{\ell m} \end{aligned} \quad (40)$$

For the normal stress balance, only the sum of the elastic tractions matters

$$\tau_{j m 2}^\Sigma = \tau_{j m 2}^- + \tau_{j m 2}^+ = (\ell + 2)(\ell - 1)(\ell(\ell + 1) + \tau_0) f_{\ell m} - 4\alpha \xi_{\ell m} - (4\alpha \phi_0 + \lambda(\ell + 2)(\ell - 1)) \psi_{\ell m} \quad (41)$$

where $\tau_0 = \sigma_0 R^2 / \tilde{\kappa} - \alpha \phi_0^2 + 2\lambda \phi_0$. The traction associated with the bilayer friction, after using Eq. [35] and Eq. [32] to express $c_{\ell m 0}^+$ in terms of $\dot{\psi}_{\ell m}$, is

$$\tau_{j m 0}^b = \tau_{j m 0}^{b,-} - \tau_{j m 0}^{b,+} = 2\beta (c_{j m 0}^- - c_{j m 0}^+) = -\frac{4\beta}{\ell(\ell + 1)(1 - \phi_0^2)} \dot{\psi}_{\ell m}. \quad (42)$$

Note that $\tau_{j m 0}^{b,-} + \tau_{j m 0}^{b,+} = 0$.

In the case of a viscous area-compressible interface, the stresses obtained from Eq. [10] are [63]

$$\begin{aligned} \tau_{\ell m 0}^{v,\pm} &= \frac{1}{2} \chi_s (\ell - 1)(\ell + 2) c_{\ell m 0}^\pm + \frac{1}{2} \chi_d (-2c_{\ell m 2}^\pm + \ell(\ell + 1)c_{\ell m 0}^\pm), \\ \tau_{\ell m 2}^{v,\pm} &= \chi_d (-2c_{j m 2}^\pm + \ell(\ell + 1)c_{\ell m 0}^\pm). \end{aligned} \quad (43)$$

Using the condition for the area incompressibility Eq. [36] and Eq. [31] yields for the viscous stresses

$$\begin{aligned}\tau_{\ell m 0}^{v,\Delta} &= \frac{\ell(\ell+1)(\chi_s + \chi_d) - 2\chi_s}{1 - \phi_0^2} \dot{\psi}_{\ell m}, \\ \tau_{\ell m 0}^{v,\Sigma} &= \frac{(2\chi_s - \ell(1+\ell)(\chi_d + \chi_s))\phi_0 \dot{\psi}_{\ell m} + 2(-2 + \ell + \ell^2)\chi_s(1 - \phi_0^2)\dot{f}_{\ell m}}{(1 - \phi_0^2)\ell(\ell+1)}, \\ \tau_{\ell m 2}^{v,\Sigma} &= -\frac{2\chi_d\phi_0}{1 - \phi_0^2} \dot{\psi}_{\ell m},\end{aligned}\quad (44)$$

The condition for incompressibility, implies that $\xi_{\ell m}$ would adjust to keep $\dot{\xi}_{\ell m} = 0$; $\alpha\xi_{\ell m}$ acts as a tension counter-acting imposed stresses to keep the area elements on the neutral surface from expanding/compressing. The ‘‘tension’’ $\alpha\xi_{\ell m}$ has two contributions: one balancing the elastic membrane stresses and one balancing the viscous stresses. The elastic contribution is determined from setting $\tau_{jm0}^\Sigma = 0$ in Eq. [40]. Solving for ξ_{jm} yields

$$\xi^{el} = -\phi_0\psi_{\ell m} + \frac{(-2 + \ell(\ell+1))\lambda\phi_0}{2\alpha} f_{\ell m} \quad (45)$$

Inserting in the expression for the tangential τ_{jm0}^Δ and normal elastic stresses τ_{jm0}^Σ leads to modified elastic stresses

$$\begin{aligned}\tau_{jm0}^\Delta &= (1 - \phi_0^2)(2\alpha\psi_{jm} - \lambda(\ell+2)(\ell-1)f_{\ell m}), \\ \tau_{jm2}^\Sigma &= (\ell+2)(\ell-1)((\ell+1) + \tau_0 - 2\lambda\phi_0)f_{\ell m} - \lambda\psi_{\ell m}.\end{aligned}\quad (46)$$

The tension arising from viscous forces is obtained from the tangential stress balance

$$(\tau_{jm0}^{hd,-} + \tau_{jm0}^{hd,+}) - \tau_{jm0}^{v,\Sigma} = -2\alpha\xi_{jm}^v. \quad (47)$$

The hydrodynamic tractions are listed in Appendix D. Solving for the average density ‘‘strain’’ yields

$$\begin{aligned}\xi_{jm}^v &= -[\alpha\ell(\ell+1)(1 - \phi_0^2)]^{-1} \\ &\times \left(-(-2 + \ell + \chi(\ell-1) + 2(-2 + \ell + \ell^2)\chi_s)(1 - \phi_0^2)\dot{f}_{\ell m} \right. \\ &\left. + (\ell(1+\ell)\chi_d\phi_0 + (-2 + \ell + \ell^2)\chi_s\phi_0 + (1+2\ell)(-1 + \chi + (1+\chi)\phi_0))\dot{\psi}_{\ell m} \right)\end{aligned}\quad (48)$$

5. Shape and lipid density evolution equations

The stress boundary conditions yield the system of equations describing the shape and density dynamics.

$$\begin{aligned}(\tau_{jm2}^{hd,-} + \tau_{jm2}^{hd,+}) - \tau_{jm2}^{v,\Sigma} + 4\alpha\xi_{\ell m}^v &= \tau_{jm2}^\Sigma \\ (\tau_{jm0}^{hd,-} - \tau_{jm0}^{hd,+}) - \tau_{jm0}^{v,\Delta} + \tau_{jm0}^b - 2\alpha\phi_0\xi_{\ell m}^v &= \tau_{jm0}^\Delta\end{aligned}\quad (49)$$

The full expressions, listed in the Appendix, Eq. [E1], are well approximated by

$$\mathbf{M} \cdot \begin{pmatrix} \dot{f}_{\ell m} \\ \dot{\psi}_{\ell m} \end{pmatrix} = -\mathbf{E} \cdot \begin{pmatrix} f_{\ell m} \\ \psi_{\ell m} \end{pmatrix} \quad (50)$$

$$\begin{aligned}M_{11} &= \frac{9 + (-5 + 3\ell^2 + 2\ell^3)(\chi + 1) + 4(-2 + \ell + \ell^2)\chi_s}{\ell(\ell+1)} \\ &\approx 2\ell(\chi + 1) + 4\chi_s \quad \text{for } \ell \gg 1 \\ M_{12} = M_{21} &= 0 \\ M_{22} &= \frac{4\beta + 2\ell + 1 + (2\ell + 1)\chi + \ell(\ell+1)\chi_d + (-2 + \ell + \ell^2)\chi_s}{\ell(\ell+1)} \\ &\approx 4\beta/\ell^2 + 2\chi/\ell + (\chi_d + \chi_s) \quad \text{for } \ell \gg 1\end{aligned}\quad (51)$$

Note that in this approximation \mathbf{M}^{-1} is the Onsager matrix, implying that the cross Onsager coefficients vanish.

Noteworthy, our model is restricted to wavelengths longer than the bilayer thickness. Specifically, the high mode cutoff is $\ell_{max} = \pi R/(2d)$, and the correction due to membrane thickness introduced in Ref. [31] is negligible. Moreover, since the shortest relaxation time $t_0 \equiv 1/\hat{\omega}(\ell = \ell_{max})$ is typically at least one order of magnitude shorter than a nanosecond (i.e., $\sim 0.01 - 0.1$ ns), this finite thickness correction[31] leads to a negligible contribution to the dynamic roughness (MSD) at times $t \gtrsim 1$ ns relevant for the application to the NSE experiments.

B. Time-correlation functions

The exponential solution to Eq. [50] is found by first diagonalizing [3]

$$\mathbf{C} = \mathbf{V} \begin{pmatrix} \gamma_1 & 0 \\ 0 & \gamma_2 \end{pmatrix} \mathbf{V}^{-1}$$

where the matrix $\mathbf{C} = \mathbf{M}^{-1} \cdot \mathbf{E}$, and \mathbf{V} is the matrix of the eigenvectors of \mathbf{C} . The relaxation rates correspond to the eigenvalues of the matrix \mathbf{C} :

$$\gamma_{1,2} = \frac{1}{2} \left(C_{11} + C_{22} \mp \sqrt{(C_{11} - C_{22})^2 + 4C_{12}C_{21}} \right) \quad (52)$$

The general expressions for the decay rates γ_1 and γ_2 are complicated, but at high wavenumbers, $\ell \gg 1$

$$\gamma_1 \sim \frac{2\kappa\alpha}{\tilde{\kappa}\chi_s}, \quad \gamma_2 \sim \frac{\ell^3}{4} \quad (\text{if } \chi_s \ll 1), \quad \text{or } \gamma_2 \sim \frac{\ell^4}{4\chi_s} \quad (\text{if } \chi_s \gg 1).$$

At low wavenumbers, $\gamma_1 = \omega(\ell, \kappa, \chi_s)$, $\gamma_2 \sim \frac{\alpha\ell^2}{2\beta}$, where

$$\omega = \frac{\kappa}{\tilde{\kappa}} \left(\frac{(\ell-1)\ell(\ell+1)(\ell+2)(\ell(\ell+1) + \bar{\sigma})}{(4\ell^2 + 4\ell - 8)\chi_s + (2\ell^3 + 3\ell^2 - 5)(\chi - 1) + 4\ell^3 + 6\ell^2 - 1} \right) \quad (53)$$

For tensionless membrane and same fluids inside and outside the vesicle, $\chi = 1$, the above expression reduces to Eq. [1] in dimensional form, $\hat{\omega} = \omega/t_{\tilde{\kappa}}$. The time correlation functions are the elements of the matrix

$$\mathbf{R} = \mathbf{V} \begin{pmatrix} e^{-\gamma_1 t} & 0 \\ 0 & e^{-\gamma_2 t} \end{pmatrix} \mathbf{V}^{-1} \mathbf{E}^{-1}$$

Specifically

$$\langle f_{\ell m}(t) f_{\ell m}^*(0) \rangle = \mathbf{R}_{11} = \langle f_{\ell m}^2 \rangle (Q_{11} e^{-\gamma_1 t} + (1 - Q_{11}) e^{-\gamma_2 t}) \quad (54)$$

with

$$Q_{11} = \frac{\gamma_2 - \omega}{\gamma_2 - \gamma_1}, \quad \omega = C_{11} - \frac{E_{21}C_{12}}{E_{22}}. \quad (55)$$

where the tension is the equilibrium one. The density-density correlations

$$\langle \psi_{\ell m}(t) \psi_{\ell m}^*(0) \rangle = \mathbf{R}_{22} = \langle \psi_{\ell m}^2 \rangle (Q_{22} e^{-\gamma_1 t} + (1 - Q_{22}) e^{-\gamma_2 t}) \quad (56)$$

with

$$Q_{22} = \frac{\gamma_2 - \omega_d}{\gamma_2 - \gamma_1}, \quad \omega_d = C_{22} - \frac{E_{12}C_{21}}{E_{11}}. \quad (57)$$

The shape-density correlations

$$\begin{aligned} \langle f_{\ell m}(0) \psi_{\ell m}^*(t) \rangle &= \langle \psi_{\ell m}(0) f_{\ell m}^*(t) \rangle = \mathbf{R}_{12} \\ &= \langle f_{\ell m} \psi_{\ell m}^* \rangle (Q_{12} e^{-\gamma_1 t} + (1 - Q_{12}) e^{-\gamma_2 t}) \end{aligned} \quad (58)$$

with

$$Q_{12} = \frac{\gamma_2}{\gamma_2 - \gamma_1} \quad (59)$$

C. Mean Square Displacement and Dynamic Structure Factor

1. General

Scattering techniques, such as neutron spin echo [22], dynamic light scattering [23], X-ray photon correlation spectroscopy [24] and some flickering experiments [25, 26] measure DSF, $S(k, t)$, that is controlled by the single-point membrane mean square displacement (MSD), $\langle(\Delta h(t))^2\rangle$, and essentially captured by [3, 27, 64]

$$S(k, t) \sim \text{Exp}\left[-\frac{k^2}{2}\langle(\Delta h(t))^2\rangle\right], \quad (60)$$

where k is the scattering wavenumber (not to be confused with the undulation wavenumber $q = \ell/R$). The dimensionless membrane segment MSD at an arbitrary 3D angle $\Omega = (\theta, \phi)$, $\langle(\Delta f(t))^2\rangle \equiv \langle(f(\Omega, t) - f(\Omega, 0))^2\rangle$, is given by

$$\langle(\Delta f(t))^2\rangle = \frac{1}{2\pi} \sum_{\ell=2}^{\ell_{\max}} (2\ell + 1) (\langle|f_{\ell m}|^2\rangle - \langle f_{\ell m}(t)f_{\ell m}^*(0)\rangle). \quad (61)$$

The MSD with physical dimensions is given by $\langle(\Delta h(t))^2\rangle \equiv R^2\langle(\Delta f(t))^2\rangle$.

2. Case of relaxed lipid density

At times when the lipid density is relaxed [29], and assuming vanishing tension

$$\langle(\Delta h(t))^2\rangle \equiv R^2\langle(\Delta f(t))^2\rangle \approx \begin{cases} \frac{\Gamma[1/3]}{2\pi 4^{2/3}} \frac{k_B T}{\eta^{2/3} \kappa^{1/3}} t^{2/3} & t_0 \ll t \ll t^* \\ \frac{1}{4\sqrt{\pi}} \frac{k_B T R}{\sqrt{\kappa} \eta_s} t^{1/2} & t^* \ll t \ll \tau_R \end{cases} \quad (62)$$

where t_0 and τ_R are the shortest and longest relaxation times (respectively), $t_0 \equiv 1/\hat{\omega}(\ell = \ell_{\max})$ and $\tau_R \equiv 1/\hat{\omega}(\ell = 2)$, and the crossover time $t^* \approx \tau_R \chi_s^{-4}$. It follows that the scattering from vesicles in this time range and large scattering wavenumbers, $kR \gg 1$, would still exhibit a stretched exponential DSF

$$S(k, t) \approx S(k) \times \begin{cases} \text{Exp}[-(\Gamma_k^{ZG} t)^{2/3}] & t_0 \ll t \ll t^* \\ \text{Exp}[-(\Gamma_k^{VG} t)^{1/2}] & t^* \ll t \ll \tau_R \end{cases} \quad (63)$$

where $\Gamma_k^{ZG} \simeq (k_B T)^{3/2} k^3 / \kappa^{1/2} \eta$ is the ZG relaxation rate and the new, membrane-viscosity-controlled, relaxation rate is given by

$$\Gamma_k^{VG} \simeq \frac{(k_B T)^2 R^2}{64\pi \kappa \eta_s} k^4 \quad (64)$$

Given that t^* can be extremely short for viscous membrane vesicles with $R \sim 20 - 50$ nm, it is quite possible that the entire NSE time window is controlled by membrane viscosity. Note that this prediction for the DSF does not account for finite-size effects arising from scattering by a spherical shell [28]. In addition, since Γ_k^{VG} depends on R , polydispersity is expected to modify the decay profile. Finally, lipid density relaxation also affects the DSF decay and limits the validity of the predicted asymptotics. We explore the coupled effects of curvature and density fluctuations in the next section.

IV. RESULTS

In this section, we explore the curvature and lipid density fluctuations of a quasi-spherical vesicle. Figure 2 illustrates the relaxation dynamics for vesicles made of a typical lipid. The decay rates are computed from Eq. [52] using the material properties listed in Ref. [3].

The lipid bilayer has a low membrane viscosity; accordingly, for a GUV, $\chi_s \ll 1$. As shown in Fig. 2a, the fast ‘‘slipping’’ mode (γ_2) decays on millisecond timescale or faster, while the slow ‘‘bending’’ mode (γ_1) decays on the order of seconds. Consistently, Fig. 3a shows that lipid density relaxes with the rate of the fast mode. Since

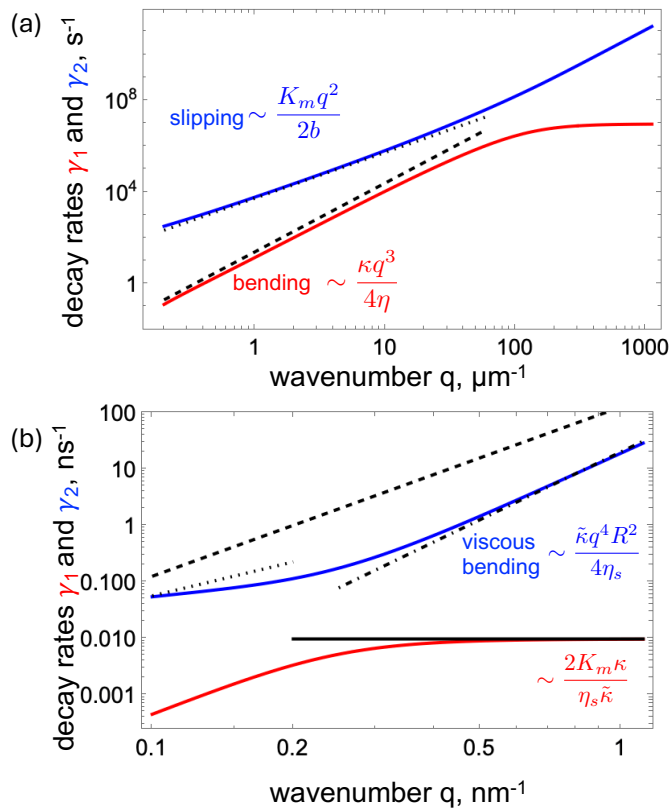


FIG. 2: Relaxation rates for vesicles made of DMPC against undulation wavenumber $q = \ell/R$: (a) a GUV with radius $R = 10 \mu\text{m}$, $\chi_s = 0.25$. (b) a SUV with radius $R = 20 \text{ nm}$, $\chi_s = 125$. Material parameters from Ref. [3], $\kappa = 13.6 k_B T$, $K_m = 0.117 \text{ N/m}$, $d = 1.4 \text{ nm}$, $b = 10^7 \text{ N.s/m}^3$, $\eta_s = 2.5 \times 10^{-9} \text{ N.s/m}$, $\chi_d = 0$, and bulk viscosity $\eta^+ = \eta^- \equiv \eta = 10^{-3} \text{ N.s/m}^2$. The black long-dashed line corresponds to the asymptotic behavior of the bending mode from the Seifert-Langer theory for a planar membrane, $\tilde{\kappa} q^3 / 4\eta$. The short-dashed line is the slipping mode, $K_m q^2 / 2b$. The solid black line is the viscous mode, $2K_m \kappa / \eta_s \tilde{\kappa}$. The dot-dashed line is the new asymptotic behavior, $\tilde{\kappa} q^4 R^2 / 4\eta_s$, for relaxation controlled by dissipation by membrane viscosity.

GUV flickering experiments usually operate at 1–1000 fps, they detect only the dynamics of the slow mode [4], and the experimentally measured bending rigidity is the thermodynamic one, κ , corresponding to relaxed lipid density. Furthermore, the bending mode relaxation rate is well-approximated by the value predicted from the planar bilayer theory, $\gamma_1 \sim \kappa q^3 / (4\eta)$ [10].

For small liposomes with $R = 20 \text{ nm}$, the system lies in the regime $\chi_s \gg 1$, and its relaxation dynamics deviate significantly from the planar membrane theory, as shown in Fig. 2b. In this case, the slow mode relaxes on a microsecond timescale, whereas the fast mode relaxes on a nanosecond timescale. Lipid density relaxation occurs on the slow-mode timescale, see Fig. 3b; consequently, membrane undulations in the sub-microsecond regime are governed by the unrelaxed bending rigidity, $\tilde{\kappa}$. Because neutron spin echo (NSE) experiments typically probe nanosecond curvature fluctuations of SUVs [8, 22], the slow mode is effectively frozen [3, 36], and the measured correlation function reflects only the relaxation of the fast mode. Unlike the planar case, however, the decay rate is slower and asymptotically scales with the fourth power of the wavenumber.

Fig. 4 illustrates the MSD behavior. Fig. 4a shows that for a GUV where the Saffman-Delbrück length is smaller than the vesicle radius, and thus $\chi_s \ll 1$, the MSD follows the ZG scaling for a planar membrane. Initially, the scaling is with $\tilde{\kappa}$, since the lipid density is unrelaxed. As time progresses, the lipid density difference relaxes and the MSD approaches the ZG asymptotic scaling with κ . The crossover region is broad since different modes relax at different rate. However, for the small liposome with radius 20nm, and thus $\chi_s \gg 1$, see Fig. 4b, no regions of clear power-law evolution exist. This is because of the fast dynamics – the crossover times, t_0 , t^* , and t_R are too close to one another; hence, the separation between the crossover times is too small for the membrane relaxation to reach the asymptotic behavior. The inset of Fig. 4b illustrates the crossover in the MSD evolution from a regime controlled by $\tilde{\kappa}$ to one governed by the relaxed bending rigidity κ . The crossover is sensitive to membrane viscosity and bilayer slip (see Fig. 5). Increasing the intermonolayer friction slows the relaxation of the lipid density difference; accordingly, for $\chi_s \gg 1$ the dynamics can reach the viscous asymptotic regime governed by $\tilde{\kappa}$ (see Fig. 5a). In contrast, decreasing

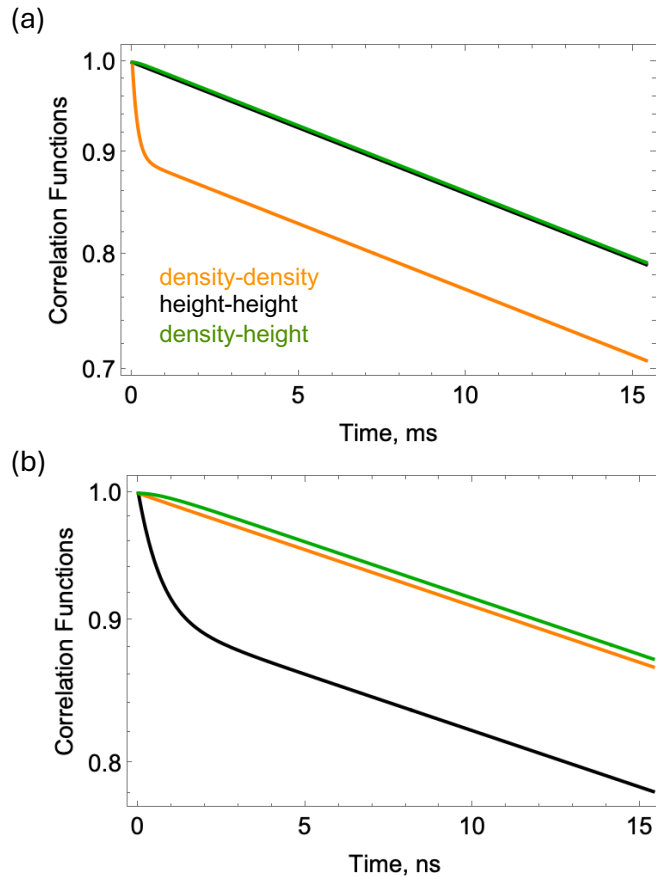


FIG. 3: Correlation functions for the curvature and density fluctuations of mode $q = 10$. (a) and (b) correspond to the same parameters as in Figs. 2(a) (GUV) and 2(b) (SUV), respectively.

the membrane viscosity (see Fig. 5b) shifts the relaxation toward the asymptotic regime described by the ZG law.

What are the implications of the new theory for the interpretation of the DSF measured by NSE experiments on liposomes? The DSF for vesicle membranes was derived in Ref.[28], and it was shown that it is well described by the MSD due to the polydispersity of the liposome suspension. Fig. 6 compares experimentally obtained values of the MSD—calculated from the DSFs (neglecting scattering finite-size effects) as [28] $\ln(S(k, t)/S(k, 0)) / (-\frac{1}{2}k^2)$ where k is the scattering wavenumber—with the theoretical prediction of Eq. [61], including the diffusional correction, $\langle \Delta f^2 \rangle R^2 + 2Dt$ (the importance of properly correcting for diffusion has been discussed in Ref. [28, 65]). Using the MD-reported viscosity [54] (interpolated to room temperature), $\eta_s \simeq 2 \times 10^{-10}$ N·s/m, versus the viscosity measured for GUVs [53] (via the vesicle electrodeformation method), $\eta_s \simeq 1 \times 10^{-8}$ N·s/m, we find that the experimental data appear to be better described by an intermediate viscosity value. This suggests a possible scale dependence of the membrane 2D shear viscosity.

Fig. 6 illustrates that the data can also be fit using the ZG model, yielding results that may appear reasonable but are, in fact, physically inconsistent. The ZG model with the correction for liposome center-of-mass diffusion yields unphysically large bending rigidity ($\sim 15\tilde{\kappa}$). However, the uncorrected ZG model produces a bending rigidity that is misleadingly close to the expected “unrelaxed” value. The present theory, which consistently incorporates diffusion effects, provides an accurate description of the data without any assumptions for the bending rigidity being “relaxed” or “unrelaxed”. This also demonstrates that fitting NSE data with the ZG model without accounting for translational diffusion can be misleading, particularly for smaller vesicles.

V. CONCLUSIONS AND OPEN QUESTIONS

We theoretically analyze the spontaneous, thermally-driven shape fluctuations of a quasi-spherical vesicle made of a single component lipid bilayer. We derive an analytical description of the dynamics of the shape and lipid density

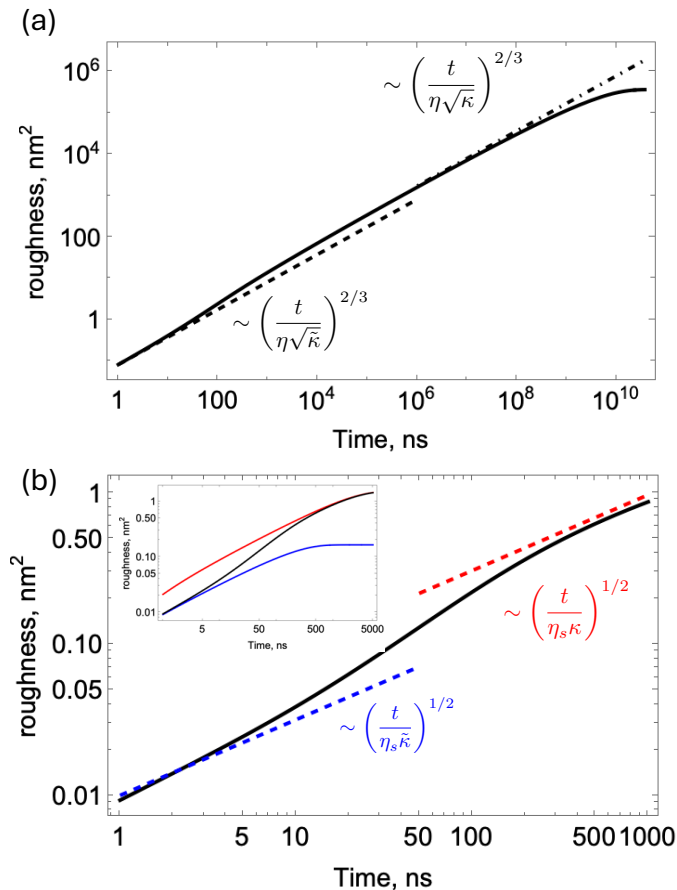


FIG. 4: Single-point membrane MSD (roughness) of vesicles. (a) and (b) correspond to the same parameters as in Figs. 2(a) (GUV) and 2(b) (SUV), respectively. The inset in (b) compares the MSD computed from the new theory (black) with that from the single-relaxation-time theory of Ref. [29], given by Eq. [1], using the relaxed bending rigidity κ (red) and the unrelaxed bending rigidity $\tilde{\kappa}$ (blue).

fluctuations with account of membrane viscosity thus extending the previous work by Miao et al. [33]. The new theory provides a unified description of the membrane dynamics in the broad time regime and wavelength spectrum spanning from cell-sized giant vesicles with radii of tens of microns down to the highly curved submicron liposomes.

We find that if the Saffman-Delbrück length η_s/η is comparable to or bigger than the vesicle radius R , membrane viscosity significantly affects the curvature fluctuations of liposomes compared to planar bilayers. Not only the membrane viscosity significantly reduces the relaxation of the bending mode, but also the asymptotic behavior of the decay rate and the DSF depart strongly from the Seifert-Langer and Zilman-Granek scalings, respectively. Furthermore, our analysis shows that curvature slows down the lipid density difference relaxation, and the DSF may not approach a stretched-exponential asymptotic behavior on the time scales of a typical NSE experiment (0.1-1000 ns). Accordingly, force-fitting the MSD with the ZG power law would lead to an overestimation of the unrelaxed bending rigidity $\tilde{\kappa}$. The effect of membrane viscosity is significant despite the uncertainty in its value (macroscopic experiments report $\eta_m \sim 10^{-9}$ N·s/m [53], whereas molecular dynamics simulations [54, 55] predict much lower viscosities.) Only for very large liposomes and low-viscosity membranes do size and viscosity effects diminish, allowing curvature fluctuations to be well described by the ZG theory. A comprehensive comparison between theory and NSE experiments will be addressed in future work.

We hope our findings will stimulate further studies into the effect of surface viscosity on the dynamics of membranes and other complex interfaces.

Conflicts of interest

There are no conflicts to declare.

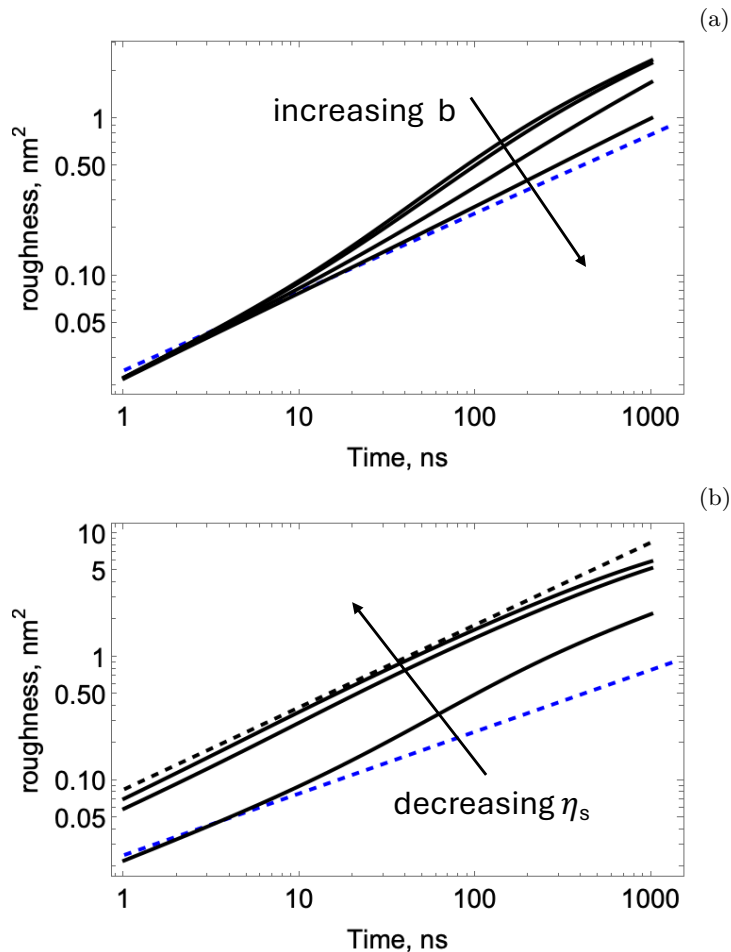


FIG. 5: Effect of bilayer slip (a) and membrane viscosity (b) on the single-point membrane MSD (roughness) of a vesicle with radius 50nm. Material parameters same as in Fig. 2, except (a) bilayer slip of increasing value: $b=10^4, 10^7, \text{ to } 10^8, 10^9 \text{ N.m}^3/\text{s}$, and (b) membrane viscosity decreasing from $\eta_s = 2.5 \times 10^{-9}$ to 20×10^{-11} to $8 \times 10^{-11} \text{ N.s/m}$ (values reported from molecular dynamics simulations [54]). The black dashed line is the ZG asymptote, and the blue dashed line is the viscous asymptote Eq. [62], both evaluated with the unrelaxed bending rigidity $\tilde{\kappa}$.

Data availability

The codes to generate the Figures are available upon request from the authors.

Acknowledgments

This research was supported by BSF Grant 2024173, and in part by the National Science Foundation under Grant NSF PHY-1748958. We thank Elizabeth Kelley, Ingo Hoffmann, and Michihiro Nagao for sharing the data for Figure 6 and for many helpful discussions.

Appendix A: Spherical harmonics

The normalized spherical scalar harmonics are defined as

$$Y_{\ell m}(\theta, \varphi) = \left[\frac{2\ell+1}{4\pi} \frac{(\ell-m)!}{(\ell+m)!} \right]^{\frac{1}{2}} (-1)^m P_{\ell}^m(\cos \theta) e^{im\varphi}, \quad (\text{A1})$$

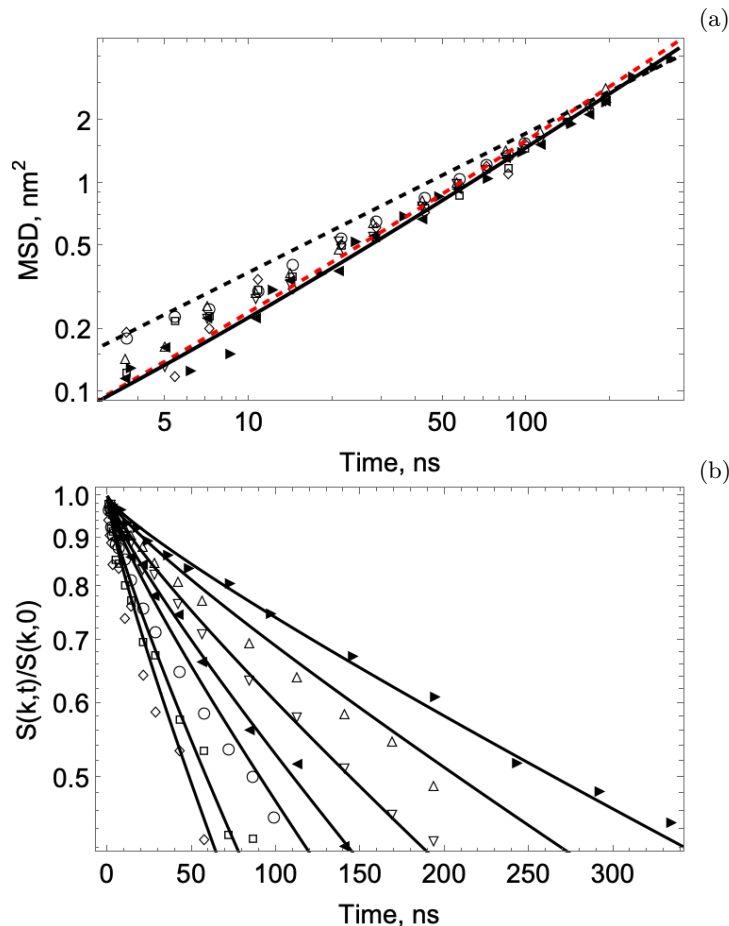


FIG. 6: (a) MSD calculated from the experimental DSFs for POPC liposomes with radius 48nm [28]. using membrane parameters $\kappa = 25k_B T$, $K_m = 122 \text{ N/m}^2$, $d = 1.45 \text{ nm}$ [28], and $b = 5 \times 10^7 \text{ N.s/m}^3$ [49]. The black solid line corresponds to the new theory with membrane viscosity $7 \times 10^{-10} \text{ N.s/m}$. The black dashed line is the ZG-asymptote not corrected for liposome center-of-mass diffusion, Eq. [62], using the “unrelaxed” bending rigidity $\tilde{\kappa}$. The red dashed line is the ZG-asymptote with diffusional correction and effective bending rigidity $15\tilde{\kappa}$. (b) Comparison between the experimental and theoretical DSFs for scattering wavenumbers from 0.63 nm^{-1} to 1.3 nm^{-1} , illustrating a good agreement for the long-time relaxation.

where $\hat{\mathbf{r}} = \mathbf{r}/r$, (r, θ, φ) are the spherical coordinates, and $P_\ell^m(\cos \theta)$ are the associated Legendre polynomials. We define vector spherical harmonics as

$$\begin{aligned}
 \mathbf{y}_{\ell m 0} &= r \nabla Y_{\ell m} = \frac{\partial Y_{\ell m}}{\partial \theta} \hat{\boldsymbol{\theta}} + i m \frac{Y_{\ell m}}{\sin \theta} \hat{\boldsymbol{\varphi}}, \\
 \mathbf{y}_{\ell m 1} &= -i \hat{\mathbf{r}} \times \mathbf{y}_{\ell m 0} = -m \frac{Y_{\ell m}}{\sin \theta} \hat{\boldsymbol{\theta}} - i \frac{\partial Y_{\ell m}}{\partial \theta} \hat{\boldsymbol{\varphi}}, \\
 \mathbf{y}_{\ell m 2} &= \hat{\mathbf{r}} Y_{\ell m}.
 \end{aligned} \tag{A2}$$

Appendix B: The equilibrium state

We choose ρ_0 as in Ref. [33], which sets $\bar{\phi}$ to zero at equilibrium. If we assume the equilibrium density of each monolayer to be the same, it should be $\hat{\rho}_0 = N^\pm/A^\pm$; $\rho_0 = \hat{\rho}_0(1 + d^2/R^2)$.

At equilibrium, if we assume unstressed sphere, $H = -1/R$, $A_- = A_0(1 + d/R)^2$ and $A_+ = A_0(1 - d/R)^2$, $\rho_0^\pm = \rho_0(1 \mp 2d/R)$ (to a linear order in d/R)

$$\phi_0 = \frac{\rho_0^- - \rho_0^+}{2\rho_0} = 2d/R, \quad \bar{\phi}_0 = \frac{\rho_0^- + \rho_0^+}{2\rho_0} - 1 = 0$$

The energy of a spherical vesicle is

$$\mathcal{H}/A_0 = 2\tilde{\kappa}/R^2 + K_m \phi_0^2 - 4K_m(d/R)\phi_0 = 2\kappa/R^2$$

showing that the contributions from the elastic energy of the monolayers cancel.

Appendix C: Variation of the energy and membrane stresses

Splitting the energy Eq. [3] into the contributions of each monolayer

$$\mathcal{H}^\pm = \frac{\tilde{\kappa}}{4} \int (2H)^2 dA + \frac{\sigma_0}{2} \int dA + \frac{K_m}{2} \int (\phi^\pm)^2 dA \mp 2dK_m \int H\phi^\pm dA. \quad (C1)$$

To find the stresses, we consider the energy change upon variation of the interface $\delta \mathbf{r} = \Psi \mathbf{n} + \Phi^i \mathbf{e}_i$. We use the following relations [66]

$$\begin{aligned} \delta(dA) &= dA (-2H\Psi + \nabla_i \Phi^i), \quad \delta H = (2H^2 - K_G) \Psi + \frac{1}{2} \nabla^2 \Psi + \Phi^i \nabla_i H \\ \delta(HdA) &= dA \left(H\nabla_i \Phi^i - K_G \Psi + \frac{1}{2} \nabla^2 \Psi + \Phi^i \nabla_i H \right) \end{aligned} \quad (C2)$$

Following [33], we consider the number of molecules associated with any local area element dA of a monolayer should be conserved under the shape variation of the monolayer

$$\delta(\rho^\pm dA) = 0 \quad (C3)$$

Thus we find the variation of the density fields

$$\delta\phi^\pm = -(1 + \phi^\pm) (-2H\Psi + \nabla_i \Phi^i) \quad (C4)$$

Accordingly

$$\delta\left((\phi^\pm)^2 dA\right) = (\phi^\pm)^2 \delta(dA) + (2\phi^\pm \delta\phi^\pm) dA = (-2H\Psi + \nabla_i \Phi^i) \left(-(\phi^\pm)^2 - 2\phi^\pm\right) \quad (C5)$$

This amounts to renormalizing the monolayer's tension

$$\sigma^\pm = \frac{1}{2} \sigma_0 - K_m \phi^\pm - \frac{1}{2} K_m (\phi^\pm)^2 \quad (C6)$$

The variation of the curvature-density coupling

$$\delta(\phi^\pm HdA) = \phi^\pm \delta(HdA) + \delta(\phi^\pm) HdA \quad (C7)$$

$$\delta \int \phi^\pm HdA = \int dA \left(\left(\phi^\pm (2H^2 - K_G) + 2H^2 + \frac{1}{2} \nabla_s^2 \phi^\pm \right) \Psi + (\phi^\pm + 1) \nabla_s H \right) \quad (C8)$$

$$\delta \int H^2 dA = \int dA (2H(H^2 - K_G) + \nabla^2 H) \Psi \quad (C9)$$

$$\delta \int \sigma dA = \int dA \sigma (-2H\Psi + \nabla_i \Phi^i) = - \int dA (2H\sigma + \nabla_s \sigma) \quad (C10)$$

after integration by parts and dropping the boundary terms.

Another way to find the variation is to consider a small deformation about a sphere [67], $r = R(r_0 + f)$, $\phi = \phi_0 + \psi$, $\bar{\phi} = \xi$. Using the shape function $F = r - R(r_0 + f)$,

$$\mathbf{n} = \frac{\nabla F}{|\nabla F|} = \frac{\hat{\mathbf{r}} - \nabla f}{\sqrt{1 + (\nabla f)^2}} \quad (C11)$$

The Jacobian, $dA = Jd\Omega$, $J = r^2/(\mathbf{n} \cdot \hat{\mathbf{r}})$ is

$$J = R^2(r_0 + f)^2 \sqrt{1 + (\nabla_s f)^2} \approx R^2(r_0^2 + 2f + f^2 + \frac{1}{2}(\nabla_s f)^2) + h.o.t. \quad (C12)$$

$$\begin{aligned}
-2H &= \nabla_s \cdot \mathbf{n} \approx \nabla_s \cdot \left(\left(\hat{\mathbf{r}} - \frac{\nabla_s f}{r} \right) \left(1 - \frac{1}{2} \frac{(\nabla_s f)^2}{r^2} \right) \right) \\
&= \nabla \cdot \hat{\mathbf{r}} - \nabla_s \cdot \left(\frac{\nabla_s f}{r} \right) - \frac{1}{2} \nabla_s \cdot \left(\frac{(\nabla_s f)^2}{r^2} \hat{\mathbf{r}} \right) \\
&= \frac{2}{r} - \frac{\nabla_s^2 f}{r^2} \\
&= \frac{2}{R} \left(r_0 - f - \frac{1}{2} \nabla_s^2 f + f^2 + f \nabla_s^2 f \right)
\end{aligned} \tag{C13}$$

$$(2H)^2 = \frac{4}{R^2} \left(r_0^2 - 2f - \nabla_s^2 f + 3f^2 + \frac{1}{4} (\nabla_s^2 f)^2 + 3f \nabla_s^2 f \right) \tag{C14}$$

$$(2H)^2 J = 4 \left(1 - \nabla_s^2 f + f \nabla_s^2 f + \frac{1}{2} (\nabla_s f)^2 + \frac{1}{4} (\nabla_s^2 f)^2 \right) \tag{C15}$$

$$(2H)J = -R \left(2r_0 + 2f - \nabla_s^2 f + (\nabla_s f)^2 \right) \tag{C16}$$

On a sphere $f = f_{\ell m} Y_{\ell m}$, $r_0 = R(1 - \frac{1}{4\pi} |f_{\ell m}|^2)$. Note that $\nabla f = \nabla_s f / r$ and $\nabla_s \cdot (r^{-2} Y_{\ell m} \hat{\mathbf{r}}) = 0$. Expanding in spherical harmonics $\nabla_s f = \sqrt{j(j+1)} f_{jm} Y_{\ell m}$, $\nabla_s^2 f = -\ell(\ell+1) f_{\ell m} Y_{\ell m}$

The f_{00} amplitude is related to the other amplitudes because of conservation of vesicle volume and it can be shown [68, 69] that

$$\begin{aligned}
V &= \frac{4\pi}{3} \left(1 + \frac{f_{00}}{\sqrt{4\pi}} \right)^3 + \sum_{\ell \geq 2} \sum_{m=-\ell}^{\ell} f_{\ell m} f_{\ell m}^*, \\
f_{00} &\approx -\frac{1}{\sqrt{4\pi}} \sum_{\ell \geq 2} \sum_{m=-\ell}^{\ell} f_{\ell m} f_{\ell m}^*,
\end{aligned} \tag{C17}$$

where $f_{\ell m}^* = (-1)^m f_{\ell -m}$. Thus $V = 4\pi/3 + O(\varepsilon^2)$ and at linear perturbation order, $O(\varepsilon)$, volume is conserved. The excess area Δ is also preserved to a leading order

$$\begin{aligned}
\Delta &= A/R^2 - 4\pi = \int \frac{(1+f)^2}{\hat{\mathbf{r}} \cdot \mathbf{n}} \sin \theta d\theta d\varphi - 4\pi \\
&= \sum_{\ell m} \frac{(\ell+2)(\ell-1)}{2} f_{\ell m} f_{\ell m}^* + O(\varepsilon^3),
\end{aligned} \tag{C18}$$

where $\sum_{\ell m} \equiv \sum_{\ell \geq 2} \sum_{m=-\ell}^{\ell}$. The outward normal vector to the vesicle surface defined by a shape function $F = r - 1 - f(\theta, \varphi, t)$ is

$$\mathbf{n} = \frac{\nabla F}{|\nabla F|} = \hat{\mathbf{r}} - \sum_{jm} \sqrt{\ell(\ell+1)} f_{\ell m} \mathbf{Y}_{\ell m 0} + O(\varepsilon^2) \tag{C19}$$

Accordingly, the mean curvature

$$H = -\frac{1}{2} \nabla \cdot \mathbf{n} = -1 - \frac{1}{2} \sum_{\ell m} (-2 + \ell(\ell+1)) f_{jm} Y_{\ell m} + O(\varepsilon^2) \tag{C20}$$

where we used the fact that $\nabla \cdot \hat{\mathbf{r}} = 2/r = 2(1 - \varepsilon f) + O(\varepsilon^2)$ and $\nabla_s^2 Y_{\ell m} = -\ell(\ell+1) Y_{\ell m}$ on a unit sphere. The Gaussian curvature to a leading order in the deviation from a sphere is

$$K_G = 1 + \sum_{\ell m} (-2 + \ell(\ell+1)) f_{jm} Y_{\ell m} \tag{C21}$$

The product of the vector spherical harmonics is recoupled as

$$\mathbf{Y}_{\ell_1 m_1 0} \cdot \mathbf{Y}_{\ell_2 m_2 0} = \chi(\ell_1, \ell_2, j) \zeta(\ell_1, \ell_2, \ell, m_1, m_2, m) Y_{\ell m} \quad (\text{C22})$$

where

$$\chi(\ell, \ell_1, \ell_2) = \frac{j(\ell+1) + \ell_1(\ell_1+1) - \ell_2(\ell_2+1)}{2[\ell(\ell+1)\ell_1(\ell_1+1)]^{1/2}}, \quad (\text{C23})$$

and the Clebsch-Gordan coefficient is

$$\zeta(\ell, \ell_1, \ell_2, m, m_1, m_2) = (-1)^{m_2} \left[\frac{(2\ell+1)(2\ell_1+1)(2\ell_2+1)}{4\pi} \right]^{\frac{1}{2}} \times \begin{pmatrix} \ell & \ell_1 & \ell_2 \\ 0 & 0 & 0 \end{pmatrix} \begin{pmatrix} \ell & \ell_1 & \ell_2 \\ m & m_1 & -m_2 \end{pmatrix}. \quad (\text{C24})$$

$\begin{pmatrix} \ell & \ell_1 & \ell_2 \\ m & m_1 & m_2 \end{pmatrix}$ is the Wigner $3j$ -symbol. A special case for the $3j$ -symbol is

$$\begin{pmatrix} \ell & \ell & 0 \\ m & -m & 0 \end{pmatrix} = \frac{(-1)^{\ell-m}}{\sqrt{2\ell+1}}, \quad (\text{C25})$$

Thus The Jacobian expansion up to third order is

$$\begin{aligned} J &= \frac{(r_0 + f_{\ell m} Y_{\ell m})^2}{\mathbf{n} \cdot \hat{\mathbf{r}}} \\ &= r_0^2 \left(1 + \frac{1}{2} \varepsilon^2 \sum f_{\ell_1 m_1} f_{\ell_2 m_2} \chi(\ell_1, \ell_2, \ell_3) \zeta(\ell_1, \ell_2, \ell_3, m_1, m_2, m_3) Y_{\ell_3 m_3} \right) \\ &\quad + 2r_0 f_{\ell m} Y_{\ell m} + \sum f_{\ell_1 m_1} f_{\ell_2 m_2} \zeta(\ell_1, \ell_2, \ell_3, m_1, m_2, m_3) Y_{\ell_3 m_3} + \dots \end{aligned} \quad (\text{C26})$$

Integration over a sphere requires

$$\int Y_{jm} Y_{j_1 m_1}^* d\Omega = \delta_{jj_1} \delta_{mm_1} \quad \text{and} \quad \int Y_{jm} d\Omega = \sqrt{4\pi} \delta_{j0} \delta_{m0} \quad (\text{C27})$$

It will kill all terms except the ones for which $m_1 = -m_2 \equiv m$, $j_1 = j_2 \equiv j$, $j_3 = 0$, and $m_3 = 0$.

$$A/R^2 = \int \frac{(r_0 + \varepsilon f_{\ell m} Y_{\ell m})^2}{\mathbf{n} \cdot \hat{\mathbf{r}}} d\Omega = 4\pi r_0^2 + \left[\frac{1}{2} f_{\ell m}^2 \ell(\ell+1) + f_{j m}^2 \right] + \dots \quad (\text{C28})$$

where we have taken into account that

$$\zeta(\ell, \ell, \ell, m, -m, 0) = \frac{1}{\sqrt{4\pi}} \quad (\text{C29})$$

The expansion for r_0 truncated at second order is given by

$$r_0 = 1 - \frac{1}{4\pi} f_{\ell m}^2 \quad (\text{C30})$$

and accordingly

$$r_0^2 = 1 - 2\frac{1}{4\pi} f_{\ell m}^2 + \dots \quad (\text{C31})$$

so from $A/R^2 = 4\pi + \Delta$ we have for the excess area

$$\Delta = f_{\ell m}^2 \left[\frac{1}{2} j(j+1) - 1 \right] \quad (\text{C32})$$

The change in the tension energy

$$\delta \left(\sigma_0 \int dA \right) = \frac{1}{2} R^2 \sigma_0 f_{\ell m}^2 (\ell(\ell+1) - 2)$$

For the other energies from Eq. [C14] and the expression for the Jacobian

$$\begin{aligned} \frac{1}{2} \int (2H)^2 dA &= 8\pi + \left(-\ell(\ell+1) + \frac{1}{2}\ell(\ell+1) + \frac{1}{4}(\ell(\ell+1))^2 \right) f_{\ell m}^2 \\ &= 8\pi + \frac{1}{2}\ell(\ell+1)(\ell(\ell+1)-2) f_{\ell m}^2 \end{aligned} \quad (\text{C33})$$

$$\int (2H)\phi dA = -R(\phi_0(8\pi + (-2 + \ell(\ell+1))f_{jm}^2) + \psi_{\ell m} f_{\ell m}^*(\ell(\ell+1)+2)) \quad (\text{C34})$$

$$\int (\phi)^2 dA = R^2 \left(\phi_0^2 \left(4\pi + \frac{1}{2}(\ell(\ell+1)-2)f_{jm}^2 \right) + 4\phi_0\psi_{\ell m} f_{\ell m}^* + \psi_{\ell m}^2 \right) \quad (\text{C35})$$

The change in the energy due to the shape and density fluctuations is

$$\begin{aligned} \delta E_\ell &= \frac{1}{2}\tilde{\kappa}(\ell(\ell+1)-2)(\ell(\ell+1)+\bar{\sigma})f_{\ell m}^2 \\ &\quad + K_m R^2(\psi_{\ell m}^2 + \xi_{\ell m}^2) - 2K_m dR\psi_{\ell m} f_{\ell m}(\ell(\ell+1)-2) \end{aligned} \quad (\text{C36})$$

where

$$\bar{\sigma} = \sigma_0 + \alpha\phi_0^2 - 2\lambda\phi_0.$$

If $\phi_0 = 2d/R$, then $\alpha\phi_0^2 = \lambda\phi_0$ and the tension $\bar{\sigma} = \sigma_0 - \alpha\phi_0^2$. This is consistent with the definition Eq. [C6]. When adding the tensions of the two monolayers, at equilibrium $\phi^- + \phi^+ = 0$, and the second term is $\frac{K_m}{4}(\phi^- - \phi^+)^2$. At equilibrium on a sphere $\phi^\pm = A_0(1 \mp d/R)^2$.

Appendix D: Fundamental set of velocity fields, tractions, and solution for the flow around a sphere

The velocity basis functions that are regular at infinity are

$$\begin{aligned} \mathbf{u}_{\ell m 0}^- &= \frac{1}{2}r^{-j-2}((2-\ell)r^2 + \ell)\mathbf{y}_{\ell m 0} + \frac{1}{2}r^{-\ell-2}\ell(\ell+1)(r^2-1)\mathbf{y}_{\ell m 2}, \\ \mathbf{u}_{\ell m 1}^- &= r^{-(\ell-1)}\mathbf{y}_{\ell m 1}, \\ \mathbf{u}_{\ell m 2}^- &= \frac{1}{2}r^{-\ell-2}\left(\frac{\ell-2}{\ell+1}\right)(1-r^2)\mathbf{y}_{\ell m 0} + \frac{1}{2}r^{-j}(\ell+(2-\ell)r^2)\mathbf{y}_{\ell m 2}. \end{aligned} \quad (\text{D1})$$

The velocity basis functions that are regular at the origin are

$$\begin{aligned} \mathbf{u}_{\ell m 0}^+ &= \frac{1}{2}r^{\ell-1}(-(\ell+1) + (\ell+3)r^2)\mathbf{y}_{\ell m 0} - \frac{1}{2}r^{\ell-1}\ell(\ell+1)(1-r^2)\mathbf{y}_{\ell m 2}, \\ \mathbf{u}_{\ell m 1}^+ &= r^\ell\mathbf{y}_{\ell m 1}, \\ \mathbf{u}_{\ell m 2}^+ &= \frac{1}{2}r^{\ell-1}\left(\frac{3+\ell}{j}\right)(1-r^2)\mathbf{y}_{\ell m 0} + \frac{1}{2}r^{\ell-1}(\ell+3-(\ell+1)r^2)\mathbf{y}_{\ell m 2}. \end{aligned} \quad (\text{D2})$$

On a sphere $r = 1$ these velocity fields reduce to the vector spherical harmonics defined by Eq. [A2]

$$\mathbf{u}_{jmq}^\pm = \mathbf{y}_{jmq}. \quad (\text{D3})$$

Hence the continuity of normal velocity becomes simply

$$c_{jm2}^+ = c_{jm2}^- \quad (\text{D4})$$

The hydrodynamic tractions on a sphere due to the velocity fields Eq. [D1] and Eq. [D2] are

$$\begin{aligned} \tau_{\ell m 0}^{\text{hd},+} &= \chi\left(- (2\ell+1)c_{\ell m 0}^+ + \frac{3}{\ell}c_{\ell m 2}^+\right), \\ \tau_{\ell m 1}^{\text{hd},+} &= -\chi(\ell-1)c_{\ell m 1}^+, \\ \tau_{\ell m 2}^{\text{hd},+} &= \chi\left(3(\ell+1)c_{\ell m 0}^+ - \frac{3+\ell+2\ell^2}{\ell}c_{\ell m 2}^+\right), \end{aligned} \quad (\text{D5})$$

$$\begin{aligned} \tau_{\ell m 0}^{\text{hd},-} &= -(2\ell+1)c_{\ell m 0}^- + \frac{3}{\ell+1}c_{\ell m 2}^-, \\ \tau_{\ell m 1}^{\text{hd},-} &= -(\ell+2)c_{\ell m 1}^-, \\ \tau_{\ell m 2}^{\text{hd},-} &= 3\ell c_{\ell m 0}^- - \frac{4+3\ell+2\ell^2}{\ell+1}c_{\ell m 2}^-. \end{aligned} \quad (\text{D6})$$

Appendix E: Evolution equations

The full expressions for the evolution equations are

$$\mathbf{A} \cdot \begin{pmatrix} \dot{f}_{\ell m} \\ \dot{\psi}_{\ell m} \end{pmatrix} = -\mathbf{B} \cdot \begin{pmatrix} f_{\ell m} \\ \psi_{\ell m} \end{pmatrix} + \mathbf{F} \quad (\text{E1})$$

where \mathbf{F} is the thermal noise or external forcing (e.g., due to applied flow and electric field).

$$A_{11} = \frac{(4 + 3\ell^2 + 2\ell^3) + (-5 + 3\ell^2 + 2\ell^3)\chi + 4(-2 + \ell + \ell^2)\chi_s}{\ell(\ell + 1)} \quad (\text{E2a})$$

$$A_{12} = \frac{((2 + \ell)(1 - \phi_0) - (\ell - 1)\chi(1 + \phi_0) - 2(2\ell(\ell + 1)\chi_d + (-2 + \ell + \ell^2)\chi_s)\phi_0)}{\ell(\ell + 1)(1 - \phi_0^2)} \quad (\text{E2b})$$

$$A_{21} = \frac{(2 + \ell)(1 - \phi_0) - 2(-2 + \ell + \ell^2)\chi_s\phi_0 - (\ell - 1)\chi(1 + \phi_0)}{\ell(\ell + 1)} \quad (\text{E2c})$$

$$A_{22} = \frac{(4\beta + (2\ell + 1)((\phi_0 - 1)^2 + \chi(\phi_0 + 1)^2) + (\ell(\ell + 1)\chi_d + (-2 + \ell + \ell^2)\chi_s)(\phi_0^2 + 1))}{\ell(\ell + 1)(1 - \phi_0^2)} \quad (\text{E2d})$$

$$\begin{aligned} B_{11} &= (\ell - 1)(\ell + 2)(\ell(\ell + 1) + \bar{\sigma}) \\ B_{12} &= -(\ell - 1)(\ell + 2)\lambda, \\ B_{21} &= -(\ell - 1)(\ell + 2)\lambda(1 - \phi_0^2), \\ B_{22} &= 2\alpha(1 - \phi_0^2). \end{aligned} \quad (\text{E3})$$

The tension $\bar{\sigma} = \sigma_0 - \alpha\phi_0^2$.

The diagonal elements of the matrix \mathbf{A} are much larger than the off-diagonal ones and the latter can be approximated by zero; for the parameters in Ref.[3] the error in the relaxation rates is size-dependent (it increases with liposome radius), but below 0.5% for modes above 20, see Figure 7. The corresponding error in the roughness for the 50nm, 100nm and 1 μ m liposomes is below 2%, 1% and 0.01%, respectively.

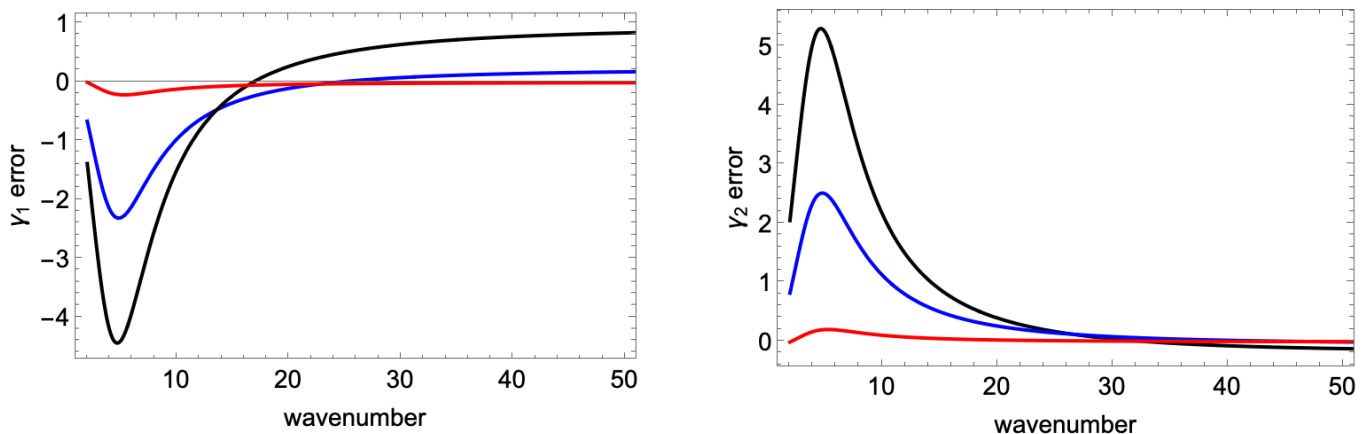


FIG. 7: Relative error (in percents) in the relaxation rates computed using the approximate, Eq. [51] and Eq. [25], and full expressions, Eq. [E2] and Eq. [E3], as a function of the wave number q for liposomes with radii $R = 50\text{nm}$ (black), 100nm (blue), and $1\mu\text{m}$ (red).

In the case of $\phi_0 = 0$ and $\chi = 1$, the asymptotic behavior of \mathbf{A} for high $\ell \gg \chi_s \gg 1$ yields the Seifert-Langer theory for a tensionless membrane $\sigma_0 = 0$ [32, 46]

$$\begin{aligned} A_{11} &\approx 4\ell, & A_{22} &\approx \ell^{-2}(4\beta + 4\ell + \ell^2(\chi_s + \chi_d)), & A_{12} &= A_{21} \approx 0 \\ E_{11} &\approx \ell^4, & E_{12} = E_{21} &\approx -\ell^2\lambda, & E_{22} &\approx 2\alpha. \end{aligned}$$

-
- [1] Patricia Bassereau, Rui Jin, Tobias Baumgart, Markus Deserno, Rumiana Dimova, Vadim A Frolov, Pavel V Bashkirov, Helmut Grubmüller, Reinhard Jahn, H Jelger Risselada, Ludger Johannes, Michael M Kozlov, Reinhard Lipowsky, Thomas J Pucadyil, Wade F Zeno, Jeanne C Stachowiak, Dimitrios Stamou, Artù Breuer, Line Lauritsen, Camille Simon, Cécile Sykes, Gregory A Voth, and Thomas R Weigl. The 2018 biomembrane curvature and remodeling roadmap. *Journal of Physics D: Applied Physics*, 51(34):343001, jul 2018.
- [2] F. Brochard and J. F. Lennon. Frequency spectrum of the flicker phenomenon in erythrocytes. *J. Phys.(France)*, 36:1035–1047, 1975.
- [3] M. C. Watson, Y. Peng, Y. Zheng, and F. L. H. Brown. The intermediate scattering function for lipid bilayer membranes: From nanometers to microns. *J. Chem. Phys.*, 135:194701, 2011.
- [4] Hammad A. Faizi, Cody J. Reeves, Vasil N. Georgiev, Petia M. Vlahovska, and Rumiana Dimova. Fluctuation spectroscopy of giant unilamellar vesicles using confocal and phase contrast microscopy. *Soft Matter*, 16:8996–9001, 2020.
- [5] John Hjort Ipsen, Allan Grønhoj Hansen, and Tripta Bhatia. Vesicle fluctuation analysis. In Rumiana Dimova and C. Marques, editors, *The Giant Vesicle Book*, page 13. CRC Press, 1st edition, 2019.
- [6] R. Dimova. Recent developments in the field of bending rigidity measurements on membranes. *Adv. Coll. Int. Sci.*, 208:225–234, 2014.
- [7] Sudipta Gupta and Rana Ashkar. The dynamic face of lipid membranes. *Soft Matter*, 17:6910–6928, 2021.
- [8] Michihiro Nagao and Hideki Seto. Neutron scattering studies on dynamics of lipid membranes. *Biophysics Reviews*, 4(2):021306, 05 2023.
- [9] C Monzel and K Sengupta. Measuring shape fluctuations in biological membranes. *Journal of Physics D: Applied Physics*, 49(24):243002, may 2016.
- [10] Brochard, F. and Lennon, J.F. Frequency spectrum of the flicker phenomenon in erythrocytes. *J. Phys. France*, 36(11):1035–1047, 1975.
- [11] Youhei Fujitani. Dynamics of the lipid-bilayer membrane taking a vesicle shape. *Physica A: Statistical Mechanics and its Applications*, 203(2):214–242, 1994.
- [12] P. Olla. The behavior of closed inextensible membranes in linear and quadratic shear flows. *Physica A*, 278:87–106, 2000.
- [13] S. B. Rochal, V. L. Lorman, and G. Mennessier. Viscoelastic dynamics of spherical composite vesicles. *Phys. Rev. E*, 71:021905, 2005.
- [14] Mark L. Henle and Alex J. Levine. Hydrodynamics in curved membranes: The effect of geometry on particulate mobility. *Phys. Rev. E*, 81:011905, Jan 2010.
- [15] Francis G. Woodhouse and Raymond E. Goldstein. Shear-driven circulation patterns in lipid membrane vesicles. *Journal of Fluid Mechanics*, 705:165–175, 2012.
- [16] Mohammad Rahimi, Antonio DeSimone, and Marino Arroyo. Curved fluid membranes behave laterally as effective viscoelastic media. *Soft Matter*, 9:11033–11045, 2013.
- [17] Mohammad Rahimi. *Shape dynamics and lipid hydrodynamics of bilayer membranes: modeling, simulation and experiments*. PhD thesis, Universitat Politècnica de Catalunya, 2013.
- [18] Jon Karl Sigurdsson and Paul J. Atzberger. Hydrodynamic coupling of particle inclusions embedded in curved lipid bilayer membranes. *Soft Matter*, 12:6685–6707, 2016.
- [19] Petia M. Vlahovska. Electrohydrodynamics of drops and vesicles. *Annu. Rev. Fluid Mech.*, 51: 305–330, 2019.
- [20] Amaresh Sahu, Alec Glisman, Joël Tchoufag, and Kranthi K. Mandadapu. Geometry and dynamics of lipid membranes: The scriven-love number. *Phys. Rev. E*, 101:052401, May 2020.
- [21] S. T. Milner and S. A. Safran. Dynamical fluctuations of droplet microemulsions and vesicles. *Phys. Rev. A*, 36:4371–4379, 1987.
- [22] Michihiro Nagao, Elizabeth G. Kelley, Rana Ashkar, Robert Bradbury, and Paul D. Butler. Probing elastic and viscous properties of phospholipid bilayers using neutron spin echo spectroscopy. *The Journal of Physical Chemistry Letters*, 8(19):4679–4684, 2017. PMID: 28892394.
- [23] E Freyssingeas and D Roux. Quasi-elastic light scattering study of highly swollen lamellar and “sponge” phases. *JOURNAL DE PHYSIQUE II*, 7(6):913–929, JUN 1997.
- [24] P. Falus, M. A. Borthwick, and S. G. J. Mochrie. Fluctuation dynamics of block copolymer vesicles. *Phys. Rev. Lett.*, 94:016105, Jan 2005.
- [25] T. Betz and C. Sykes. Time resolved membrane fluctuation spectroscopy. *Soft Matter*, 8:5317–5326, 2012.
- [26] E. Helffer, S. Harlepp, L. Bourdieu, J. Robert, F. C. MacKintosh, and D. Chatenay. Microrheology of biopolymer-membrane complexes. *Phys. Rev. Lett.*, 85:457–460, 2000.
- [27] A. G. Zilman and R. Granek. Undulations and dynamic structure factor of membranes. *Phys. Rev. Lett.*, 77:4788–4791, Dec 1996.
- [28] Rony Granek, Ingo Hoffmann, Elizabeth G. Kelley, Michihiro Nagao, Petia M. Vlahovska, and Anton Zilman. Dynamic structure factor of undulating vesicles: finite-size and spherical geometry effects with application to neutron spin echo experiments. *EUROPEAN PHYSICAL JOURNAL E*, 47(2), FEB 2024.
- [29] Hammad A Faizi, Rony Granek, and Petia M Vlahovska. Curvature fluctuations of fluid vesicles reveal hydrodynamic dissipation within the bilayer. *Proceedings of the National Academy of Sciences*, 121(44):e2413557121, 2024.
- [30] Frank Heinrich and John F Nagle. The effect of cholesterol on the bending modulus of dopc bilayers: re-analysis of nse data. *Soft Matter*, 21(12):2258–2267, 2025.

- [31] Zachary G. Lipel, Yannick A. D. Omar, and Dimitrios Fraggadakis. Finite membrane thickness influences hydrodynamics on the nanoscale. *Phys. Rev. Fluids*, 10:103101, Oct 2025.
- [32] U. Seifert and S.A. Langer. Viscous modes of fluid bilayer membranes. *Europhys. Lett.*, 23:71–76, 1993.
- [33] L. Miao, M. A. Lomholt, and J. Kleis. Dynamics of shape fluctuations of quasi-spherical vesicles revisited. *Eur. Phys. J. E.*, 9:143–160, 2002.
- [34] T V Sachin Krishnan, Kento Yasuda, Ryuichi Okamoto, and Shigeyuki Komura. Thermal and active fluctuations of a compressible bilayer vesicle. *Journal of Physics: Condensed Matter*, 30(17):175101, apr 2018.
- [35] E. Evans and A. Yeung. Unexpected dynamics in shape fluctuations of bilayer vesicles. *J. Phys. II*, 5:1501–1523, 1995.
- [36] M. C. Watson and F. L. H. Brown. Interpreting membrane scattering experiments at the mesoscale: The contribution of dissipation within the bilayer. *J. Chem. Phys.*, 98:L9–L11, 2010.
- [37] R. Rodríguez-García, L. R. Arriaga, M. Mell, L. H. Moleiro, I. López-Montero, and F. Monroy. Bimodal spectrum for the curvature fluctuations of bilayer vesicles: Pure bending plus hybrid curvature-dilation modes. *Phys. Rev. Lett.*, 102:128101, Mar 2009.
- [38] Éric Freyssingeas, Didier Roux, and Frédéric Nallet. Quasi-elastic light scattering study of highly swollen lamellar and “sponge” phases. *Journal de Physique II*, 7(6):913–929, 1997.
- [39] U. Seifert. Configurations of fluid membranes and vesicles. *Advances in physics*, 46:13–137, 1997.
- [40] D. E. Discher and F. Ahmed. Polymersomes. *Annu. Rev. Biomed. Eng.*, 8:323–341, 2006.
- [41] E. Evans and R. Skalak. *Mechanics and Thermodynamics of Biomembranes*. CRC Press, Boca Raton, Florida, 1980.
- [42] T.R. Powers, G. Huber, and R.E. Goldstein. Fluid-membrane tethers: Minimal surfaces and elastic boundary layers. *Phys. Rev. E*, 65:041901, 2003.
- [43] U. Seifert. Fluid membranes in hydrodynamic flow fields: Formalism and an application to fluctuating quasispherical vesicles in shear flow. *The European Physical Journal B - Condensed Matter and Complex Systems*, 8(3):405–415, Apr 1999.
- [44] E. Evans, A. Yeung, R. Waugh, and J. Song. Dynamic coupling and nonlocal curvature elasticity in bilayer membranes. In *The Structure and Conformation of Amphiphilic Membranes*, volume 66, pages 148–153. Springer Proceedings in Physics, 1992.
- [45] E. Evans and A. Yeung. Hidden dynamics in rapid changes of bilayer shape. *Chem. Phys. Lipids*, 73:39–56, 1994.
- [46] Jean-Baptiste Fournier. On the hydrodynamics of bilayer membranes. *International Journal of Non-Linear Mechanics*, 75:67–76, 2015. Instabilities and Nonlinearities in Soft Systems: From Fluids to Biomaterials.
- [47] W. K. den Otter and S. A. Shkulipa. Intermonolayer friction and surface shear viscosity of lipid bilayer membranes. *Biophysical Journal*, 93:423–433, 2007.
- [48] R. Merkel, E. Sackmann, and E. Evans. Molecular friction and epitactic coupling between monolayers in supported bilayers. *J. Phys France*, 50:1535–1555, 1989.
- [49] Autumn A. Anthony, Osman Sahin, Murat Kaya Yapici, Daniel Rogers, and Aurelia R. Honerkamp-Smith. Systematic measurements of interleaflet friction in supported bilayers. *BIOPHYSICAL JOURNAL*, 121(15):2981–2993, AUG 2 2022.
- [50] D. A. Edwards, H. Brenner, and D. T. Wasan. *Interfacial Transport Processes and Rheology*. Butterworth-Heinemann, Boston, 1991.
- [51] D. A. Edwards and D. T. Wasan. Surface rheology ii. the curved fluid surface. *J. Rheology*, 32:447–472, 1988.
- [52] BU Felderhof. Effect of surface elasticity on the motion of a droplet in a viscous fluid. *The Journal of chemical physics*, 125(12), 2006.
- [53] Hammad A. Faizi, Rumiana Dimova, and Petia M. Vlahovska. A vesicle microrheometer for high-throughput viscosity measurements of lipid and polymer membranes. *BIOPHYSICAL JOURNAL*, 121(6):910–918, MAR 15 2022.
- [54] James E. Fitzgerald, Richard M. Venable, Richard W. Pastor, and Edward R. Lyman. Surface viscosities of lipid bilayers determined from equilibrium molecular dynamics simulations. *BIOPHYSICAL JOURNAL*, 122(6):1094–1104, MAR 21 2023.
- [55] Andrew Zgorski, Richard W. Pastor, and Edward Lyman. Surface shear viscosity and interleaflet friction from nonequilibrium simulations of lipid bilayers. *Journal of Chemical Theory and Computation*, 15(11):6471–6481, 2019. PMID: 31476126.
- [56] R. Dimova, C. Dietrich, A. Hadjiisky, K. Danov, and B. Pouligny. Falling ball viscosimetry of giant vesicle membranes: Finite-size effects. *EUROPEAN PHYSICAL JOURNAL B*, 12(4):589–598, DEC 1999.
- [57] R. Dimova, S. Aranda, N. Bezlyepkina, V. Nikolov, K. A. Riske, and R. Lipowsky. A practical guide to giant vesicles. probing the membrane nanoregime via optical microscopy. *J. Phys. Cond. Matt.*, 18:S1151–S1176, 2006.
- [58] Eduardo Guzmán, Javier Tajuelo, Juan Manuel Pastor, Miguel Ángel Rubio, Francisco Ortega, and Ramón G. Rubio. Shear rheology of fluid interfaces: Closing the gap between macro- and micro-rheology. *Current Opinion in Colloid & Interface Science*, 37:33–48, 2018. Surface analysis techniques.
- [59] A. Ponce-Torres, J. M. Montanero, M. A. Herrada, E. J. Vega, and J. M. Vega. Influence of the surface viscosity on the breakup of a surfactant-laden drop. *Phys. Rev. Lett.*, 118:024501, Jan 2017.
- [60] P. M. Vlahovska and R.S. Gracia. Dynamics of a viscous vesicle in linear flows. *Phys. Rev. E*, 75:016313, 2007.
- [61] Petia M. Vlahovska. Dynamics of membrane bound particles: capsules and vesicles. In C. Duprat and H.A. Stone, editors, *Low-Reynolds-Number Flows: Fluid-Structure Interactions*. Royal Society of Chemistry Series RSC Soft Matter, 2016.
- [62] R.E. Goldstein, P. Nelson, T. Powers, and U. Seifert. Front propagation in the pearling instability of tubular vesicles. *J. Phys. II France*, 6:767–796, 1996.
- [63] J. T. Schwalbe, F. R. Phelan, P. M. Vlahovska, and S. D. Hudson. Interfacial effects on droplet dynamics in poiseuille

- flow. Soft Matter, 7:7797–7804, 2011.
- [64] Anton G. Zilman and Rony Granek. Membrane dynamics and structure factor. Chemical Physics, 284(1):195–204, 2002. Strange Kinetics.
- [65] Ingo Hoffmann, Elizabeth G Kelley, Michihiro Nagao, Petia Vlahovska, and Rony Granek. Describing neutron spin echo data from undulating lipid vesicles: recent advances. Applied Crystallography, 59(1), 2026.
- [66] Markus Deserno. Fluid lipid membranes: From differential geometry to curvature stresses. Chemistry and physics of lipids, 185:11–45, 2015.
- [67] Wolfgang Helfrich. Size distributions of vesicles: the role of the effective rigidity of membranes. Journal de Physique, 47(2):321–329, 1986.
- [68] U. Seifert. Fluid membranes in hydrodynamic flow fields: Formalism and an application to fluctuating quasispherical vesicles. Eur. Phys. J. B, 8:405–415, 1999.
- [69] P. Vlahovska, J. Bławdziewicz, and M. Loewenberg. Deformation of a surfactant-covered drop in a linear flow. Phys. Fluids, 17:Art. No.103103, 2005.